Czech University of Life Sciences in Prague

Faculty of Environmental Sciences

Department of Environmental Geosciences

Czech University of Life Sciences Prague

Cadmium adsorption onto Fe and Mn oxides – Implications for Cd isotopic fractionation

Diploma Thesis

Thesis Supervisor: prof. RNDr. Michael Komárek, Ph.D.

Consultant: Ing. Zuzana Vaňková, Ph.D.

Author: B.Sc. Nasrin Moradikoochi

2022

CZECH UNIVERSITY OF LIFE SCIENCES IN PRAGUE

Faculty of Environmental

DIPLOMA THESIS ASSIGNMENT

B.Sc. Nasrin Moradikoochi

Environmental Geosciences

Thesis title:

Cadmium adsorption onto Fe and Mn oxides – Implications for Cd isotopic fractionation

---

Objectives of thesis

The aim of the review part of the Master thesis is to summarize basic concepts and knowledge concerning Cd and its occurrence in the environment, stable metal isotopes, adsorption processes, and studies dealing with isotopic fractionation of Cd during adsorption onto various solid phases.
In the experimental part of the thesis, the kinetics of Cd adsorption and isotopic fractionation during complexation with two different Fe oxides, ferrihydrite and goethite, will be investigated. Based on the obtained adsorption and isotopic fractionation equilibrium times, Cd adsorption edges onto both Fe oxides will be determined. Cd isotopic fractionation will be measured using thermal ionization mass spectrometry (TIMS).

Methodology:

The work will consist of:
1) Literature research
2) Batch sorption experiments involving Cd and ferrihydrite and goethite
3) Analytical procedures (ICP-OES, TIMS analyses)

The proposed extent of the thesis: 50 pages

Keywords

Cadmium, adsorption, isotopic fractionation, ferrihydrite, goethite

Recommended Information Sources:

1. Essington, M. E. (2004). Soil and Water Chemistry: An Integrative Approach. CRC Press. Boca Ranton.
2. Horner, T. J., Rickaby, R. E., Henderson, G. M. (2011). Isotopic fractionation of cadmium into calcite. Earth and Planetary Science Letters, 312(1–2), 243–253.
3. Post, J.E. (1999). Manganese oxide minerals: Crystal structures and economic and environmental significance. Proceedings of the National Academy of Sciences USA, 96, 3447-3454.
4. Wasylenki, L. E., Swihart, J. W., Romaniello, S. J. (2014). Cadmium isotope fractionation during adsorption to Mn oxyhydroxide at low and high ionic strength. Geochimica et Cosmochimica Acta, 140, 212–226.
5. Wiederhold, J. G. (2015). Metal stable isotope signatures as tracers in environmental geochemistry. Environmental Science & Technology, 49(5), 2606–2624.

Expected date of thesis defence

2021/22 SS - FES

The diploma supervisor

prof. RNDr. Michael Komarek, Ph.D.

The diploma consultant

Ing. Zuzana Vaňková, Ph.D.

Electronically approved: 3. 11. 2020
prof. RNDr. Michael Komárek, Ph.D.
Head of department

Electronically approved: 24. 11. 2020
prof. RNDr. Vladimír Bejček, CSc.
Dean

Prague on 29. 03. 2022

Declaration

I hereby declare that I have independently written this diploma thesis titled "*Cadmium adsorption onto Fe and Mn oxides – Implications for Cd isotopic fractionation*" under the supervision of prof. RNDr. Michael Komárek, Ph.D. and consultant of Ing. Zuzana Vaňková, Ph.D. I have listed the all the literature and publications from which I have acquired information in the reference section.

In Prague, Czech Republic of 2022

X

Nasrin Moradikoochi Bc.S.

Acknowledgments

I would like to extend my gratitude to my dedicated thesis advisor prof. RNDr. Michael Komarek Ph.D. who was always available for consultation and conferences regarding research topics and reviewing. I would like to extend my appreciation to Ing. Zuzana Vaňková, Ph.D., my consultant, for through recommendations and gracious help. Lastly, I would like to thank my family, friends, and colleagues for their endless encouragement as well as proofreading and editing final drafts of this work. All of this would not have been possible without them. My sincerest thanks.

Nasrin Moradikoochi

Abstract

Cadmium is a naturally occurring element, but it is also found in higher concentrations in the environment as a result of anthropogenic activity. Cadmium is potentially toxic to the environment, so it is critical to identify the pathways of these contaminants that may be present in the environment. Instrument and technology advancements, such as TIMS development (Thermal Ionization Mass Spectrometry) and MC-ICP-MS (Multi-Collector Inductively Coupled Plasma Mass Spectrometry), have enabled the analysis of non-traditional isotopes. Cadmium isotopes have traditionally been challenging to analyze in terms of isotopic fractionation. To determine the processes by which this element becomes isotopically enriched or depleted in the different environments, it is critical to understand how it reacts with soil phases and in an aqueous solution.

The primary goal of this thesis was to determine the effect of pH and ionic strength on Cd adsorption as well as the adsorption and isotopic kinetics of Cd onto two different Fe oxides the present in soil, ferrihydrite, and goethite. For our experiment, we chose synthetic ferrihydrite and goethite as representatives. The study's main goal was to provide a more in-depth understanding of the interaction between the surface chemistry of each soil phase and Cd. Experiments were conducted to create adsorption edges of $1x10^{-4}$ M Cd solutions with various ionic strengths of 0.1M, 0.01M, and 0.001M $NaNO_3$. Adsorption was assessed by varying the pH of each solution over a progressive pH values in an inert atmosphere. The adsorption of Cd was highly dependent on the specific mineral phase; it is worth noting that the effect of pH on each mineral adsorption varied depending on the element, implying that while Cd shares similar properties, it behaves differently. Furthermore, the adsorption and isotopic kinetics of Cd onto ferrihydrite and goethite has reached equilibrium in the 24 hours of times intervals, and according to acquired results, the isotopic kinetic of adsorption onto goethite was faster than ferrihydrite.

According to the results of the experiments, Cd fractionation during adsorption was more significant in the adsorption onto ferrihydrite, the $\delta^{114/112}$Cd values for the 24 hour time interval has shown values at the corresponding standard deviation: i.e., 0.372 ± 0.025‰ for ferrihydrite and 0.106 ± 0.014‰ for goethite. Meanwhile, there was no discernible effect of solution ionic strength on ferrihydrite adsorbed Cd. Adsorption of Cd onto goethite reached equilibrium (89%) in 30 minutes, whereas ferrihydrite adsorption reached its peak (98%) after 24 hours. The results implied that a 24-hour equilibration time is sufficient to achieve both adsorption and kinetic equilibrium.

Keywords: cadmium, adsorption, isotopic fractionation, ferrihydrite, goethite

Table of Contents

1 Introduction

Pollution of the environment is a continuing issue. It is described as the discharge of substances into the environment that may harm human and animal lives, ecosystems. Soil operates as a significant sink for toxins, collecting large amounts of pollution from various anthropogenic and natural sources, such as industrial activity, waste disposal, sewage outflow, and volcanic activity. Because soil formation takes longer than human life, it should be viewed as a finite, non-renewable natural resource on which humankind is predicated and performs productive, ecological, and social roles in the landscape ecosystem (Farmer 1997).

Mining, wastes disposal, pesticide application, and fossil fuel burning are all familiar sources of metal pollution. Metals, unlike organic molecules, do not dissolve over time; therefore, the soil may become contaminated with potentially harmful metals. Cadmium is a common metal found in contaminated sites. The behavior of Cd is of great interest in the realm of geochemistry and, more specifically, in this project. Cadmium is a highly toxic element in the soil environment, this element may exist in natural states in mineral constituents or through anthropogenic insertion due to pollution (Alejandro et Paloma Raquel Aragon 2012). The total anthropogenic emission in 1983 was 7570 (t/year). The share of anthropogenic sources of Cd in an environment, can be measured by enrichment factor and if the enrichment factor is larger than 10, the Cd in the sample can be from an anthropogenic origin (Feska et al. 2021).

Cadmium aerosols can be released into the environment as a result of its industrial transformation (Chrastný et al. 2015). Fly ashes from smelter stack which containing quickly soluble metal elements such as Cd, which can contaminate the soil and threaten the agricultural soil's health (Komarek et al. 2009). Since the 1980s, the mobilization and emission of Cd from anthropogenic sources are 5000 times higher than the natural weathering sources. Consequently, a significant amount of Cd has been released to the

atmosphere, sediment, and aquatic environment relative to the initial concentration in the continental crust (Ratie et al. 2021). In the following, we discuss different biogeochemistry characteristics of Cd.

1.1 Aim of this thesis

This thesis aims to summarize the biogeochemistry behavior of Cd, the basic concepts concerning their stable metal isotopes in the environment, and the analytical methods used to determine isotopic fractionation. The application of these topics will be observed from their application to environmental geochemistry.

From an experimental point of view, this thesis aims to determine the pH-dependence of adsorption of Cd on the representative soil phases. In further studies, the adsorption edges will be evaluated for adsorption of Cd onto the soil phases and to estimate the influence of the adsorption process on the isotopic fractionation of Cd in soils.

2 Literature review

2.1 Biogeochemistry of Cd

2.1.1 Introduction to characteristics of Cd

The high toxicity of Cd has made it a highly controversial element in geochemistry field. Cadmium is regarded as one of the most environmentally hazardous metals, having negative impacts on all biological processes. Metal replacement of Zn by Cd causes toxicity in some essential enzyme molecules and inactivates them. Cadmium element located within elemental group 12B (see Table 1). Due to physiochemical properties of Cd, there are additional environmental risks involved in the Cd interactions in the environment. This element may be introduced to the environment as in mineral constituents or via anthropogenic insertion due to pollution within the range of the soil environment. The mobility of Cd cations in the soil system is determined by the soil phase and the soil ability to adsorb or bind the contaminants (Baskaran 2011; Chrastný et al. 2015). Cadmium is a post-transition metal with an atomic number of forty-eight. Fridrich Stromeyer discovered Cd in 1817 in contaminated zinc compounds which has been sold in pharmacies in Germany.

Table 1. General physio-chemical properties of Cd (Cullen et Maldonado 2013)

Chemical property	Cd
Group in periodic table	IIB
Atomic number	48
Atomic weight	112.4
Atomic radius (A°)	155
Ionic radius of Cd^{2+}	95
Electron configuration	[Kr] $4d^{10}5s^2$
Melting point (ºC)	320.9
Boiling point (ºC)	767.3
Density at 25°C (gcm^{-3})	8.642
Oxidation state	(+2), (+1, not common)

Reduction potential (E°) for $Cd^{2+} + 2e^{-} = Cd$ (V)	-4.02
First ionization energy (KJ $mol^{-}1$)	867
Second ionization energy (KJ mol^{-1})	1625
First hydrolysis constant (pKH)	10.1
Electronegativity	1.69
Solubility product of metal carbonate (-log K_{SO})	11.7
Solubility product of metal oxide and hydroxide (-log K_{SO})	14.4

2.1.2 Cd sources

Cadmium constitutes ~0.1 ppm of the Earth crust, with a total amount of Cd in the earth crust of 65 ppm, making it the 64th element in the earth crust. Two primary sources of Cd in the atmosphere are naturals and anthropogenic sources. Natural ones include volcanoes, sea salt spray, and terrestrial biomass burning, weathering the parent rocks containing Cd; they can also be from biogenic sources. On the other hand, anthropogenic sources include non-ferrous metal production, fossil fuel combustion, iron and steel production, and cement production (Conrad et al. 2007) (see Table 2). However, the anthropogenic sources of Cd are a more of significant problem, and these sources are often more unstable due to increased solubility and bio-availability (Loganthan et al. 2012).

The most abundant Cd compounds in the environment are the sulfide forms. As a fully naturally occurring mineral, Greenockite (CdS) can be mentioned, which is the mineral that is known to have the most significant proportion of Cd. Other minerals that are source of Cd are otavite ($CdCO_3$), hawleyite (CdS), ramdohrite ($Pb_{5.9}Fe_{0.1}Mn_{0.1}In_{0.1}Cd_{0.2}Ag_{2.8}Sb_{10.8}S_{24}$), and sphalerite (ZnS) in a smaller amount; also, it can be found in Pb ores as an impurity, like in galena (PbS) (Chrastný et al. 2015). Moreover, Cd has been observed in different phases and, it can be bound to inorganic (SO_4^{2-}, Cl^{-}, F^{-}, and HCO_3^{-}) and organic (fulvic and humic acids, amino acids, citrate, oxalate, salicylate) ligands (Zhang et al. 2019). Cadmium production is

tied to the processing of ores rich in Cu, Pb, and, most notably, Zn, the production of which is not dependent on Cd demands. Cadmium is commonly extracted from sphalerite (ZnS). Furthermore, Cd can be recovered as a by-product of Zn and Pb ores smelting by electrolysis, and distillation. The last study on the production of Cd in 2011 shows that China, the Republic of Korea, and Japan have the highest share in the production of Cd in the world (Zhu et al. 2015; Sposito 2008).

Table 2. Global anthropogenic and natural emissions of Cd in mid-1990s (Cullen et al. 2013).

Anthropogenic		Natural	
Source	Cd Emission (t yr^{-1})	Source	Cd Emission (t yr^{-1})
Fossil fuel combustion	691	Volcanoes	820
Non-ferrous metal production	2,171	Biogenic	240
Iron and steel production	64	Wind-born dust	210
Cement production	17	Terrestrial biomass burning	110
Waste disposal	40	Sea-salt spray	60
Total	2,983	Total	1440

2.1.3 Cadmium usage

Production of the rechargeable battery containing Ni-Cd is the primary industrial usage of Cd. The favorability of Cd-containing batteries has increased the demand for their production, and their improper disposal has increased their anthropogenic mobilization. The other usage of Cd in the technology is in pigments production for coloring plastics, inks, and rubber (Chrastný et al. 2015). Moreover, Cd became a popular metal for making sacrificial corrosion-resistant coatings for iron and steel.

Batteries, alloys, coatings (electroplating), solar cells, plastic stabilizers, and pigments are all common industrial uses for Cd today. Cadmium was utilized in batteries for 86% in 2009, mostly in rechargeable Ni-Cd batteries. In 2004, the European Union set a 0.01% restriction on Cd in electronics, with few exclusions, then in 2006, the limit was cut to 0.002%. Also, the Ag-Cd battery is another form of Cd-based battery (Strawn et al. 2020) (see Table 3). Another application of Cd is in electroplating in the aircraft industry to prevent corrosion of steel components, accounting for 6% of global output. Cadmium is a metal that can be found in semiconductor materials. Photodetectors and solar cells use Cd sulfide, Cd selenide, and Cd telluride, some motion detectors, which are sensitive to mid-infrared light. In the last 30 to 40 years, the concerns about Cd toxicity have led to the regulation and decline in the usage of Cd in the industry (Page et Bingham 1973).

Table 3. Characteristics uses, health effects of Cd (Strawn et al. 2015)

Metal:	Uses:	Health effects:
Cd	Electroplating, Cd batteries, cell-phones, lap top computers.	Carcinogenic, lung fibrosis, dyspnea, chronic lung testicular degeneration.

2.1.4 Effect of Cd on plants

Cadmium has a nutrient-like behavior due to the similarity of its behavior to Zn, and it can replace nitrate and phosphate and be a nutrient for the specific type of algae. Cadmium can replace Zn in carbonic anhydrase, which is a vital enzyme in the photosynthesis process carbon fixation of algea (Abouchami et al. 2012). Cadmium uptake by the plant and entry of Cd into the food chain is most likely due to the use of P fertilizers containing Cd. Some of the soil solution complexes of micronutrients are necessary for the plants, but they can be toxic in high concentrations (Koretsky 2000).

Cadmium pathway from soil to the plants starts from Cd desorption from the solid phase to the solution; after desorption, Cd will be uptaken by the plants and distribute in the plant internal system (Imseng et al. 2018). Cadmium poisoning in plants can impair photosynthesis, water, mineral uptake, and plant vital functions (Gallego et al. 2012). The manifestation of Cd poisoning in the plants differ from delay in growth, changes in the leaf chloroplast content, damaging the photosynthetic system, or impairing respiration (Navarro-Leon et al. 2019). One of the severe effects of Cd in a plant is the production of reactive oxygen species (ROS) (Pérez-Chaca et al. 2014). Accumulation of ROS in plants degenerates the photosystem and restrain photosynthesis (Navarro-Leon et al. 2019). Cadmium is considered as non-essential element for all environmental spheres, plants, and animals, with the exception of certain algal species (Cao et al. 2006).

2.1.5 pH and solubility of Cd

The pH of the soil is an important factor in determining Cd bioavailability, bioaccessibility, and mobility (Stigliani et al. 1991). In conducted studies for immobilization of heavy metals, the amount of soluble metals has been decreased by increasing pH, also, the precipitation ratio has been increased by the increase in pH (Houben et al. 2013). Cadmium immobilization and adsorption are reversible reactions and dependent on the soil pH; by re-acidifying the soil, Cd availability will increase in the environment (Cappuyns et al. 2008). According to several studies the pH over 6.5 decreases the availability, mobilization of metallic cations (Dziubanek et al. 2015). Many factors influence the metals solubility and mobility in the soils, such as pH, temperature, redox potential, organic matter decomposition, leaching, ion exchange, and microbial activity. Organic compounds released by the plant roots and change the soil pH affects the mobility and bioavailability of heavy metals such as Cd by several chemical processes (Liu et Huang 2005).

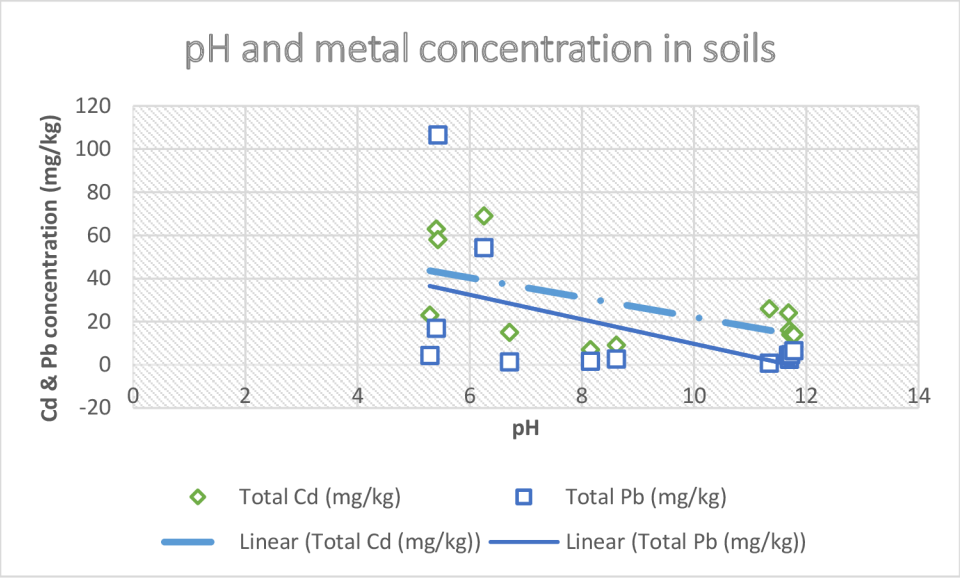

Fig. 1. Mobility of Cd in different types of soil in varied pH (Hamid et al. 2020).

2.1.6 Cadmium in water

The heavy metal in the water resources can originate from contaminated sediment and soil. The Cd source in rivers and lakes can be from the pre-industrial source. Moreover, industrial and agricultural runoff increased the level of Cd in the natural water resource (Zhang et al. 2019). The first report of disease from the contaminated water sources with Cd was from the Jinzu river in Japan which caused the Itai Itai disease in the people who have been used the contaminated water, the concentration amount of the Cd from Jinzu river has been reported at 4.85 mg/kg soil (Jiraungkoorskul et al. 2016). The standard concentration of Cd differs in different type of water resources and effluents (see Table 4).

The ocean receives the Cd that is mobilized from the crust and atmosphere. According to the study by Cullen & Maldonado (2013), the rate of solubility of the Cd in seawater is higher than 80% and it will be dissolved in 6 hours of exposure. Cadmium can be considered as a micronutrient to some groups of diatoms in the ocean. The uptake of Cd by phytoplankton is directly related to the concentration of Cd and indirectly to the concentrations of Zn, Mn, and Fe (Cullen et Maldonado 2013).

Cadmium has been complexed with natural organic matter in freshwater resources, and consequently, its toxicity has been decreased. This complexation decreases the amount of free Cd. However, the complexation of Cd with organic ligands in water is highly dependent on dissolved organic carbon, pH, and their competition in making the ligands bond with other trace cations. The toxicity of Cd to the organisms in freshwater is bound to the speciation of the metal (Cao et al. 2006).

Cadmium in halides and sulfate compounds can form different ions or complexes in the water (Mason 2013); $CdCl_2$ in the water is dissolved into Cd^{2+}, $CdCl^{+}$, $CdCl^{3-}$ ions, and consequently, they form complexes such as $CdCl_2.H_2O$ and $CdCl_2.2.5H_2O$. Furthermore, the Cd in ion form can react with water and form different complexes such as $CdOH^{+}$, $Cd(OH)_2$, $Cd(OH)_3$, $Cd(OH)_4$, and Cd_2OH^{3+}. And, in the hydrothermal situation the natural ligands that transport the Cd are OH^{-}/H_2O, Cl^{-}, and HS^{-}/H_2S.

Table 4. Standard concentration of Cd in different type of water (Kinuthia et al. 2020)

Organization/Country	Types of water	Recommended Cd limits in ppm
WHO	Drinking water	0.005
	Wastewater effluents	0.003
China (Chinese Ministry of Health; and National Standards)	Drinking water	0.005
	Wastewater effluents	0.03
Kenya (NEMA and KEBS)	Drinking water	0.01
	Wastewater effluents	0.01
US EPA	Drinking water	0.005
	Wastewater effluents	0.01
World Bank	Wastewater effluents	0.1

.

The Cd chloride complexes in aqueous solution have been studied by using X-ray diffraction (XRD), Nuclear Magnetic Resonance (NMR), Raman, Infrared, and X-ray absorption spectroscopies methods at the different temperatures and pressure. Examination of the Cd level in water has been conducted by examining the Cd level in the sediment; for instance, the Cd level of Elizabeth River in Virginia has been elevated as the result of the fossil fuel development, tested by the evaluation of the sediment of the area (Conrad et al. 2007). A thorough understanding of the distribution of Cd in water and its fractionation is needed for a better understanding of the Cd speciation is solid.

2.1.7 Cadmium in soil and rocks

Cadmium in the soil system can be absorbed, precipitated, exchanged with ions, and involved in the complexation reaction. The concentration of Cd in the soil is considered to be driven by the parent rocks. Sedimentary rocks have the highest concentration of Cd in soils of any type of rock. The majority of the Cd in the soil is in the solid phase in various chemical compounds, with only a small portion in the soil solution form, which is primarily determined by the soil pH (Imseng et al. 2018). According to Komarek et al. (2009), the majority of the Cd in the soil is in the exchangeable fraction. The phosphate fertilizers contain ions such as Ca^{2+}, PO_4^{3-}, and SO_4^{2-}, that might change the extractable and available Cd for plants in the soils (Wiggenhauser et al. 2018). The mobility and bioavailability of Cd in the soil system and soil porewater are determined by organic and inorganic ions, pH, and Cd chemical speciation. According to Komarek et al. (2009) Cd has high mobility in soil system. The study by Vanek et al. (2005), stated that Cd has a high mobility compared to Zn and Pb and it has been confirmed by the mobility factor value. The behavior of Cd in soil is determined by the metal origin and history, and a large portion of Cd in soil is derived from anthropogenic sources (Cullen et al. 1999).

Cadmium can be accumulated in the agricultural soil by several means, such as mineral phosphate fertilization, deposition from the atmosphere, compost amendment, sewage sludge, wastewater, and industry activities (Wiggenhauser et al. 2018). The majority of fertilizers are derived from phosphate rocks, which contain a significant amount of Cd sulfate; however, the initial concentration of Cd in fertilizer is not problematic; the Cd bioaccumulation behavior over the time and amount of application can cause problems. Generally, the agricultural soil standard for Cd concentration should not exceed one ppm; however, it is different in each region (see Table 5) (Adriano 2001).

Table 5. Cd concentration in agricultural soil (Adriano 2001)

Canada	0.56 ppm
England	< 1.0 ppm
Denmark	0.22 ppm
Japan	0.45 ± 0.23 ppm
United States (Western)	0.33 ppm
United States (North Central)	0.37 ppm
United States (North East)	0.17 ppm
United States (South)	0.15 ppm
World	0.40 ppm

2.1.8 Cadmium poisoning

According to the International Agency for Research on Cancer, there is no safe level of exposure for Cd, and it has been underlined in the first group of carcinogenic elements (IARC 2018). The most significant concern for humans regarding Cd toxicity is the preferential solubility of Cd as it is highly toxic to almost any species that filters or uses water within its organism (Cao et al. 2006). Cadmium concentrations in soil, air, and water are trace, and Cd poisoning is caused by Cd bio-accumulative behavior (Dziubanek et al. 2015). Cadmium has relatively high mobility and can accumulate in

the organs and tissues, which is toxic and carcinogenic in the long term (Phillips 1995). The Cd speciation can determine its bioavailability, mobility, and toxicity (Ratie et al. 2021).

Cadmium poisoning in humans can be caused by consumption of fish from contaminated water resources or agricultural products from the soil with a high level of Cd. In the northern part of Russia, contaminated rice from the rice paddies irrigated by Cd-rich water caused the fatality (Moiseenko et Gashkina 2018). Cadmium poisoning in humans also can be caused by smoking tobacco, and due to the long biological half-life (15-30 years) of Cd, chronic toxicity will arise (Robson et al. 2014). For testing the effect of Cd on the human body, liver and tissue samples need to be examined; the person should have lived in the area for at least ten years and should not have worked in industries with high Cd toxicity (Megorsky 2003). Cadmium accumulation in tissues and organ changes their function, bringing the progression of diabetes, hypertension, osteoporosis, leukemia, and neoplasms (Satarug et al. 2003; Li et al. 2011).

Cadmium has been accumulated in the liver and kidney of fishes from the contaminated area due to the high bioaccumulation of Cd. Fish from the low mineralized lakes with air-born anthropogenic pollution show high Cd concentration. It is viable that this occurred due to the similarity of Cd and Zn physiochemical properties. Cadmium is suggested to take over the Zn function in the vital organs (Moiseenko et Gashkina 2018). As a result of the P fertilizer application, the Cd accumulation in arable soils increases and transfers to the staple food products. The Cd derived from fertilizers ends up in the edible plant parts and food chain (Wiggenhauser et al. 2018). Cacao beans show a relatively high Cd level, reported from central and south America (Gramlich et al. 2018).

2.2 Cd isotopes

Isotopes are atoms that have the same number of electrons and protons but differ in neutrons. The mass number (the sum of nucleons) written as a superscript to the left of the element symbol, and the number of protons written as a subscript to the left of the element symbol, can be useful to identify atoms (Michener et Lajtha 2007). Decay is a process in which unstable nucleus results in the release of ionizing radiation in the form of a particle (alpha and beta) or electromagnetic radiation (gamma, x-radiation) and transform into a daughter isotope (possibly different element). The radioactive half-life is the time taken for half of a substance radioisotopes to decay (Kirkland 2007).

Cd isotopes have been studied since the 1970s, until now that the Cd isotopes have been used as an isotope tracer to understand the Cd geochemistry cycle, particularly for river/sediment environments. Naturally, Cd has eight isotopes, ^{106}Cd, ^{108}Cd, ^{110}Cd, ^{111}Cd, ^{112}Cd, ^{113}Cd, ^{114}Cd, ^{116}Cd. Cadmium has six stable isotopes at natural state and two naturally radioactive isotopes. According to Zhu et al. (2015) ^{114}Cd is the most abundant in the environment, around 28.7%, and ^{108}Cd with 0.89% is the least abundant. At the minimum, three isotopes ^{110}Cd, ^{111}Cd, and ^{112}Cd are stable. Among the isotopes that do not occur naturally, the most long-lived are ^{109}Cd with a half-life of 462.6 days and ^{115}Cd with 53.46 hours. The most naturally abundant stable isotopes of Cd is ^{114}Cd (see Table 6). The value of isotopes from the anthropogenic activity is distinguishable from the terrestrial source by studying the isotopes and their share. The six stable isotopes of Cd can be used in different field of studies such as marine biogeochemistry and oceanography, Cd uptake by plants and source tracing of Cd (Holden et al. 2018).

Table 6. Cd isotopes and their natural abundance (JLab ©2022)

Mass number	Natural Abundance	Half-life	Decay Mode	Branching Percentage

106	1.25%	>3.6*10^{+20} years	Double Electron Capture	No Data Available
108	0.89%	>1.9*10^{+18} years	Double Electron Capture	No Data Available
110	12.49%	Stable	-	-
111	12.80%	Stable	-	-
112	24.13%	Stable	-	-
113	12.22%	8*10^{15} years	Beta-minus Decay	100.00%
114	28.73%	>2.1*10^{18} years	Double Beta-minus Decay	No Data Available
116	7.49%	3.3*10^{+19} years	Double Beta-minus Decay	No Data Available

According to Komarek et al. (2021), Cd hydroxides contain heavier isotopes than other Cd complexes, such as Cd nitrate, Cd hydrates, or Cd chlorides, due to the tendency of lighter isotopes of Cd to adsorb onto the sorbent. Naturally, Cd does not involve in the redox reactions, the processes that can affect the Cd are precipitation, adsorption, and complexation with other minerals in the environment or organic matter presence (Ratie et al. 2021). Cadmium isotope reference material must meet four criteria in order to be representative and practical

- It is necessary to ensure a long-term supply of isotope ratio monitoring.
- It must be isotopically homogeneous, which is convenient to achieve with a solution.
- Elemental impurities should be kept to a minimum in order to avoid interfering with isotope measurements, especially for isobaric element effect.
- The Cd isotopic composition should be representative of Bulk Silicate Earth (BSE), which has been precisely characterized in comparison to in-house reference solutions.

The isotopes have been used to study in order to analyze their environmental cycle and effects. The result from the Cd isotopes analyses and its biogeochemical process can be applied to paleoceanography (Abouchami et al. 2011). Stable metal isotope analyses are one of the branches of isotopic studied, which is counted as non-traditional isotopes studies, which is categorized for studying the trace elements and potentially volatile and sensitive elements to oxidation-reduction (Baskaran 2011). The technologies such as Thermal Ionization Mass Spectrometry (TIMS), and Multi-Collector Inductively Coupled Plasma Mass Spectrometry (MC-ICP-MS) has given the ability to analyze heavier isotopes such as transition and post-transition metals (Wiederhold 2015).

The studies on the range of the Cd isotopes fractionation in various types of rocks have shown the $\varepsilon^{114/110}$Cd value for sphalerite, Smithsonite, greenockite, and otavite ranged between −2 and +3, and the results from rocks like shale, basalt, diorite is -4 to +4 (Chrastny et al. 2015). The value of $\varepsilon^{114/110}$Cd for dust (−6.4) is lower than the $\varepsilon^{114/110}$Cd value in slag (+3.6) residue from smelter activity. Furthermore, the Cd in solution is isotopically heavier than the Cd in solid phase, which may demonstrate the enrichment of light isotopes of Cd in living plant cell walls. However, fractionation during the different processes brings difficulties in isotope tracing (Komarek et al. 2021; Yang et al. 2015).

2.2.1 Isotopic fractionation of Cd

Fractionation of Cd is mass-dependent; activities such as burning coal, urban waste, smelting, metal coating, glass industry, and agriculture result in mass-dependent fractionation of Cd isotopes (Chrastný et al. 2015). According to Baskaran (2011), isotopic fractionation is related to the structural coordination of soil phase minerals. The adsorption of metallic cations in the different soil phases has resulted in the fractionation and since the Cd shows one natural oxidation state, making it more sensitive to the isotopic fractionation process (Hoefs 2015). The specific fractionation

of Cd isotopes may help identify the element transformation through their formation and, even more so, their fate within the environment. Several experimental studies on the isotopic fractionation and enrichment of one isotope in the define phase has demonstrated that the Cd tends to enrich the lighter Cd isotopes onto the adsorbed phase (Wiederhold 2015; Wombacher et al. 2003). The fractionation of Cd in the aqueous solution is not only dependent on the Cd-O bond length in liquid phase but the bond length between the Cd and organic matter for instance the bond between the Cd and thiol (R-SH) group. In interpreting the isotopes fractionation, all of the previously mentioned factors, as well as the clay mineral content of the soil, must be taken into account (Yang et al. 2015; Ratie et al. 2021; Fulda et al. 2013; Karlsson et al. 2005; Isaure et al. 2015).

The study on measuring of the Cd stable isotopic fractionation and its complexation have shown lighter isotopes favorability in adsorption. The study by Wasylenki et al. (2014), has shown the lighter Cd isotopes adsorption onto Mn-oxyhydroxide, and the study by Ratie et al. (2021) shows light isotopes of Cd complexation with humic acid. Isotopic fractionation of Cd in the adsorption process on birnessite is only observed in high ionic strength environments like seawater, which indicates that the Cd speciation in the environment can be affected by salinity which can affects its fractionation (Komarek et al. 2021). The source tracking of the Cd and its fractionation in a different process, such as evaporation and condensation during the industrial emission, can solve many environmental issues (Ratie et al. 2021).

2.2.2 Stable isotopic fractionation of Cd

Environmental science is a scientific instrument that examines toxins in the environment using various analytical techniques. In terms of risk analysis, remediation procedures, and contaminated land management, determining the scope and level of soil pollution is crucial. Stable isotope fingerprinting is one of the ways of examining the toxins and their origin in the environment. The ratios of stable isotopes variation

depends on its source. Isotope fractionation, or the depletion or concentration of one isotope relative to another, can produce distinct isotopic signatures (fingerprints). Equilibrium fractionation (e.g., complexation, dissolution, precipitation) and kinetic fractionation (e.g., diffusion, evaporation) are two types of isotope fractionation processes. Isotope fractionation can therefore be used to investigate the origins and mechanisms of metal transfer in soils. The concentration of trace elements, their mobility, and bioavailability, which can be determined using various extraction procedures such as single or sequential extraction methods or diffusive gradients in thin films technique, are also crucial in the ecotoxicological assessment of contaminated soils (Hoefs 2015; White 2014).

Isotope fractionation is caused by the different behavior of isotopes. It refers to any situation that results in different isotope distributions between two substances or between two phases of the same material with different isotope ratios. As a result, the abundances of the element stable isotopes change. It can happen as a result of biological, chemical, or physical processes. Lighter elements are more affected by isotopic fractionation than heavier elements (e.g., C, H, O, S). The two fundamental mechanisms that cause fractionation are the kinetic isotope effect and the equilibrium isotope effect. Both are mass-dependent, implying a discernible variation in the rates or levels of isotope fractionation, which is controlled by the mass variation between the atoms or molecules.

Adsorption of metallic cations by soil phases results in isotopic fractionation; Cd mostly occur in one single natural oxidation state and when it becomes complex, it is highly susceptible to isotopic fractionation (Baskaran 2011; Hoefs 2015). According to Baskaran (2011), Isotopic fractionation is closely related to the structural coordination of specific soil phase minerals. The adsorption processes associated with isotopic fractionation differ, depending on the solution state of equilibrium (Wiederhold 2015). Any environment in which adsorption processes occur and can reach an equilibrium state is highly dependent on several factors. Isotopes

fractionation can happen during the sorption, precipitation, evaporation, redox changes, plant and microorganisms interaction. The isotopic fractionation is a temperature-dependent process; isotopic fractionation decreases with the increasing temperature. In order to describe the fractionation of metals in an aqueous solution, two different perspectives have been proposed; one is studying the fractionation of metal in coexisting aqueous solution, and the other one is monitoring the isotope fractionation in between the solid (adsorbed) and aqueous species (Komarek et al. 2021; Zhao et al. 2021).

Stable isotopic fractionation of metals has been utilized as a functional tool to understand the processes associated with the specific interest. There is a variation in the number of neutrons present in its atomic structure within any isotope; consequently, each specific isotope weight differs, resulting in varying reactivity and slight discrepancies in their physicochemical properties (Hoefs 2015). Each element with numerous isotopes can be utilized in scientific research and brings the possibility of studying their environmental cycling. The stable isotopes of metals can be utilized as indicators of environmental processes studies and numerous fields such as geochemistry, cosmology, and biology (Loganthan et al. 2012).

Nevertheless, several different isotopes have varied throughout multiple different natural phenomena, which this process has not been understood well. The variety of element isotopic fractionation must be accurate relative to the given reference material in the NIST so that studies results can be compared to the baseline. The relativity of the isotopes to the reference material complicates requirements for global scientific communities due to the difficulty of acquiring reference material. An interesting trend has been shown by mechanisms involving adsorption processes to analyze the fractionation of an element isotopes. In the solution, lighter metal stable isotopes are preferentially adsorbed onto the sorbent and create the solid part of the solution, and the heavier isotopes tend to the portioning into the dissolved phase of the solution. The isotopic fractionation method, information, and data in environmental

studies apply to sources or process tracing. In the source tracing studies, the isotopic fractionation tends to define and determine the initial source of the interest isotope in the complicated known system. On the other hand, using the isotopes fractionation to trace the process tries to track the specific process transforming an isotope into the second distinguishable isotope (Wiederhold 2015; Wombacher et al. 2003).

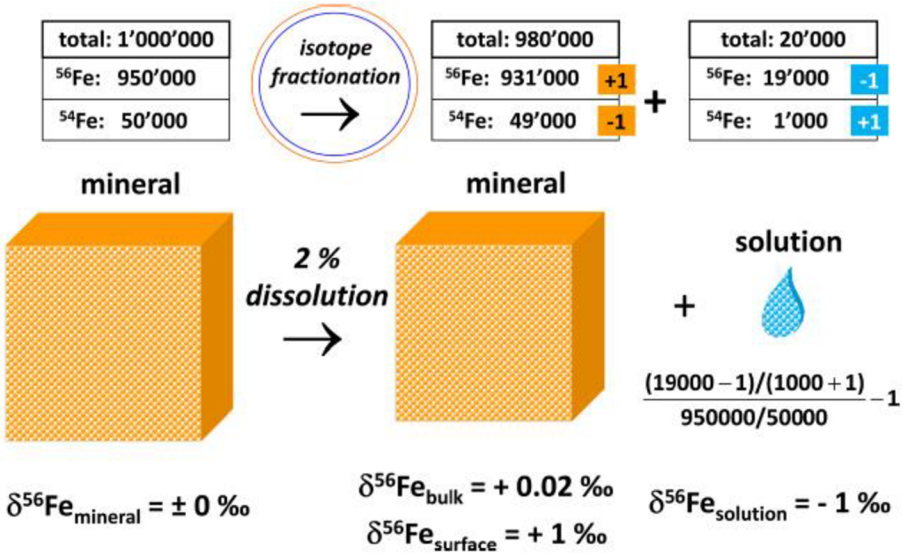

Fig.2. Example of iotopic fractionation due to mineral dissolution (Wiederhold 2015).

2.3 Mass spectrometry

Mass spectrometry (MS) is a powerful analytical technique for the determining the mass-to-charge rates of ions formed. It can be used to examine gaseous, liquid, or solid. The mass-to-charge rate (m/z) is an ad hoc measurement. Even though protons and electrons are positively and negatively charged, their numbers in an atom are equal; therefore, their charges cancel out. When the number of protons exceeds the number of electrons, the atom becomes charged. The total charge of sodium atoms, for example, is zero since they have 11 protons and 11 electrons. On the other hand, sodium ions contain 11 protons and 10 electrons; therefore, their overall charge is +1. The ion source, mass analyzer, and detector are the three essential components of a mass spectrometer. To avoid collisions with air molecules, the mass analyzer, detector, and some types of ion sources all require a vacuum; hence a pumping

system is also incorporated. After entering the instrument through the inlet, the sample is ionized in the ionization chamber before being extracted into the analyzer, which determines the ions based on their m/z. Lighter ions will be deflected more than heavier ones. Finally, detectors detect the ions, and mass spectra are recorded, giving the relative abundance of each resolved ionic species. Ionization (electrospray, chemical ionization, fast atom bombardment), separation (quadrupole, time of flight, ion trap), and detection (e.g., faraday cups, photomultipliers, microchannel plates) techniques are all available (Misra 2019).

Mass spectrometers are made up of various combinations of these techniques. Mass spectrometers commonly used for investigating the stable isotope composition of environmental materials include the gas source Isotope-ratio mass spectrometer (IRMS), multi collector inductively coupled plasma mass spectrometer (MC-ICP-MS), and thermal ionization mass spectrometer (TIMS). The mass analyzers in all of these mass spectrometers are similar, consisting of a magnetic sector (to produce a mass spectrum) and numerous Faraday cups (to gather several mass ion beams simultaneously), but they differ in sample input into the ion source and ion conversion. As a result, each instrument may be appropriate for a particular sample type (Aelion et al. 2009).

2.3.1 Isotope-ratio mass spectrometry IRMS

The term isotope-ratio mass spectrometry (IRMS) refers to mass spectrometry procedures that detect the relative abundances of multiple isotopes of a given element in a sample. It is also referred to as gas source isotopic ratios mass spectrometry. The gas source IRMS is commonly used to investigate stable isotopes of light elements (C, H, N, O, S), noble gases (He, Ne, Ar, Kr, Xe), and Si and Cl. For this procedure to work, the sample must be introduced in a gaseous state. To determine the C isotope ratios in benzene, the chemical must first be transformed into the measuring gas (e.g., CO_2). The sample gas is then compared to a reference gas

calibrated with an international isotopic reference material with a highly defined isotopic composition (Prohaska et al. 2015). In an electron ionization ion source, the injected gas molecules are ionized. The ionization process is accomplished by hitting a target with electrons. The sample intake is used to introduce a sample into the ionization chamber. An electron beam is created by heating a Re or W filament with the 70-volt electric current and collecting it in a trap electrode. The positive voltage on the repeller electrode electrically pushes produced ions out of the ion source and into the analyzer.

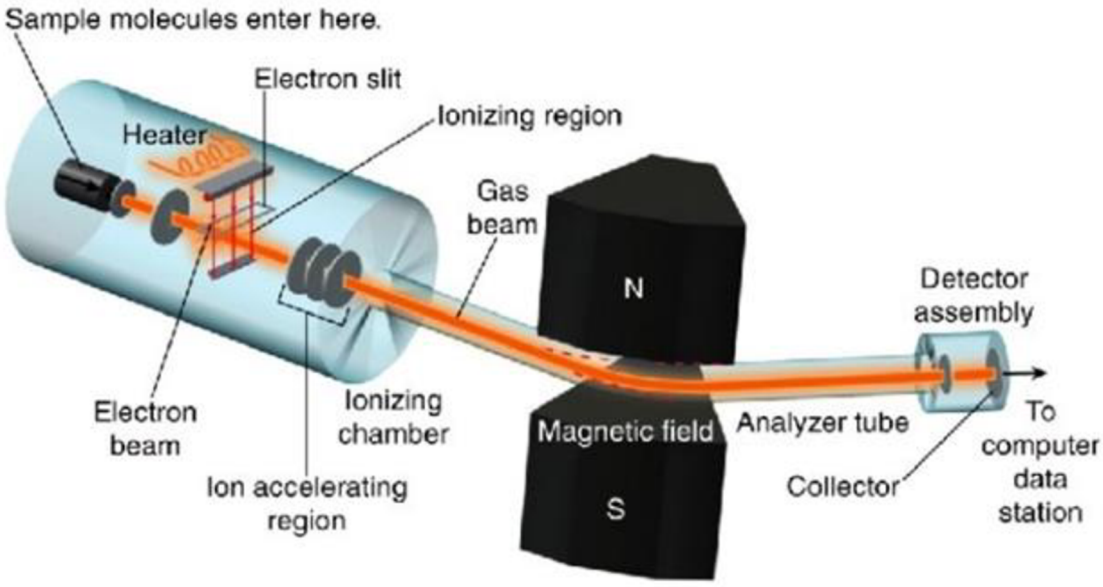

Fig.3. Scheme of an electron ionisation ion source (Jones ©2015)

2.3.2 Inductively coupled plasma mass spectrometry

Liquid samples are delivered through a nebulizer to form a fine aerosol, then transported to a high-temperature (up to roughly 7700°C) Ar plasma for inductively coupled plasma mass spectrometry (ICP-MS). Plasma is an ionized gas that atomizes and ionizes a sample by releasing positive ions and free electrons. Ions are then isolated and sent to a mass spectrometer (Wilschefski et Baxter 2019). A typical ICP-MS ion source comprises a quartz torch at the end whereby the plasma is produced and a load coil supplied by radiofrequency energy to create an oscillating magnetic

field that accelerates and decelerates the plasma ions and electrons in order to heat the plasma inductively. Several types of mass spectrometers, including sector field mass spectrometers (ICP-SFMS) and multi-collector (MC-ICP-MS) instruments, can be used with an ICP source, including sector field mass spectrometers (ICP-SFMS) and multi-collector (MC-ICP-MS) instruments, which have numerous detectors (usually Faraday cups) for simultaneous determination of ions with different masses allows the exact isotopes ratio determination (White 2017).

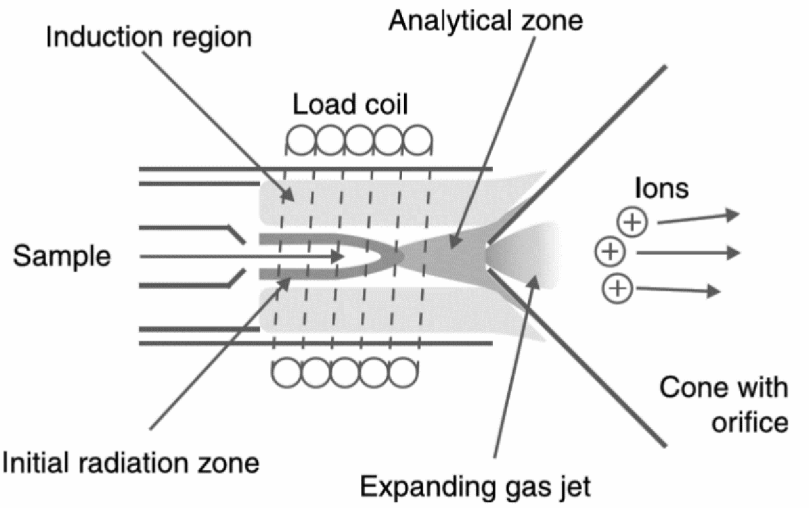

Fig.4. Inductively coupled plasma ion source scheme (Ekman et al. 2008)

In ICP-MS, an Ar plasma can ionize more than 50 elements with over 90% efficiency. Only a few elements, such as halogens, are incapable of ionizing due to their higher ionization potential than Ar (At, Br, Cl, F, I). Argon could be substituted for He to improve ionization efficiency in these circumstances. This approach is versatile and sensitive, and it has frequently been used to examine inorganic compounds, such as isotope ratios and trace element analysis (Ekman et al. 2008).

2.3.3 Thermal ionization mass spectrometry

Thermal ionization mass spectrometry (TIMS) measures the ions created when one or so more refractory metal filaments (such as Re, Ta, or W) are electrically heated to temperatures frequently surpassing 1000 °C. The triple filament source is depicted in Figure 5. In this configuration, the sample is manually put onto one of the

outside filaments that are heated to evaporate the material. The generated neutral vapor is then guided into a much hotter central filament, where it is ionized and extracted to the mass analyzer and other MS components. The efficiency of ionization is determined by the filament surface chemical and physical qualities and the filaments configuration. The triple (or double) filament supply may be far more effective than a single filament source since the evaporation and ionization processes are separated, allowing the ionization filament to reach higher temperatures. As a result, even elements with a high ionization potential could be ionized efficiently. This technique provides a highly exact, accurateand sensitive approach for determining stable isotope ratios. It is mainly used for isotope analysis and geochronology (Ekman et al. 2008).

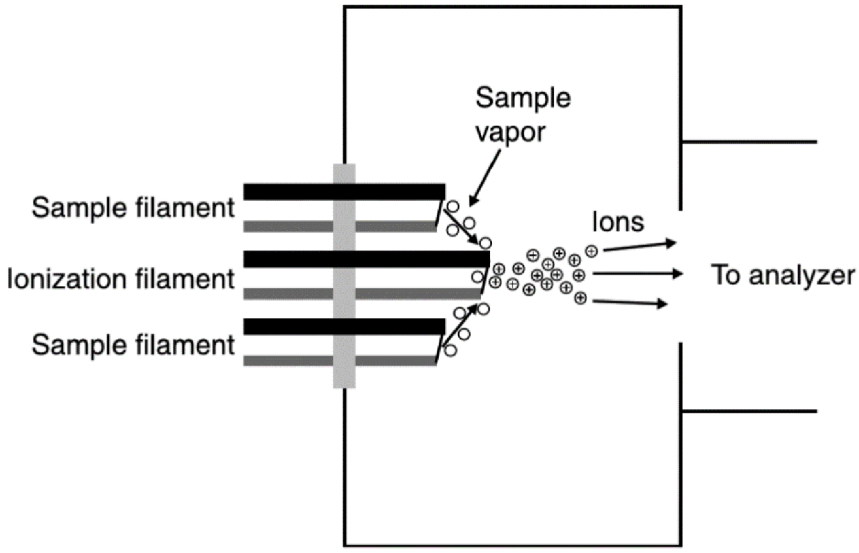

Fig .5. A schematic representation of a thermal ionization source with a triple filament configuration; each filament comprises two pins connected by a wire (Ekman et al. 2008).

The TIMS and MC-ICP-MS equipment can measure isotope ratios for a wide variety of elements with a precision of fewer than 50 parts per million. Nevertheless, TIMS isotope analysis is more time-consuming than MC-ICP-MS because the sample must be manually put onto a metal filament and thoroughly heated to obtain a stable ion beam, whereas MC-ICP-MS offers an automated sample introduction. On the other

hand, TIMS is much less likely to be affected by isotopic fractionation, which can occur in the percent range with MC-ICP-MS depending on the instrument setup and time. The TIMS and MC-ICP-MS have further distinctions, such as operating costs and component advantages (Pico 2015).

2.3.4 Mass spectrometry of isotope fractionation

Thermal ionization mass spectrometry (TIMS) or multi-collector inductively coupled plasma mass spectrometry (MC-ICP-MS) techniques quantify Cd isotope fractionation. The MC-ICP-MS and TIMAS use the magnetic field to detect and separate isotopes based on their masses (Abouchami et al. 2012; Teng et al. 2017). Thermal ionization mass spectrometry is more accurate and provides more information than MC-ICP-MS. The TIMS mass bias is low, systematic, and consistent. However, MC-ICP-MS has conducted additional research on stable metal isotopes. Nonetheless, the MC-ICP-MS mass bias can be corrected using various techniques, including I) double spike techniques and ii) external normalization to a known isotope from a different complexation that must be added to the sample prior to the analyses. iii) standard sample bracketing method, in which the mass bias of the standard is assumed to be the same as measured standards (Komarek et al. 2021). The mass bias in MC-ICP-MS techniques for determining Cd stable isotopes can be corrected by external normalization to Ag and Sb isotopes (Wombacher et al. 2003).

In the analytical process of Cd isotopes by TIMS, factors such as i) ionization sensitivity and efficiency regarding the Cd abundancy in natural samples, ii) sample output by considering the preparation and sampling process should be considered (Komarek et al. 2021). The measurement of Cd stable isotope fractionation requisite an instrument mass bias correction. Five of the seven laboratories used the double spike techniques for mass bias correction in an overview study of seven laboratory experiments on measuring stable isotope fractionation (Abouchami et al.

2012). On the other hand, only two laboratories have used sample calibrator bracketing or element doping to quantify mass bias correction.

2.4 Adsorption

2.4.1 Introduction

Surface adsorption is a selective separation method that involves transferring a specific component of the gas or liquid phase to the porous side surface. The ability of an adsorbent to selectively adsorb soluble components from a carrier fluid has led to a broader application of this process. Adsorption is the accumulation of adsorbed molecules on the adsorbent inner surface, and because only a minor amount of adsorption can occur per unit area, ultra-porous adsorbents with a flat to very high volume ratio are used. Basically, the selectivity of an adsorbent between solute and carrier fluid or between different solutes makes it possible to separate specific solvents from the carrier fluid and from each other. In a similar way, in a reverse operation called disposal, the components in the solid are separated. By adsorption, many separations can be made that are sometimes impossible or impractical by other separation techniques such as distillation, precipitation; (Burger et al. 2000), liquid-liquid extraction, and membrane separation and flotation methods (Macfarlane et al. 2009). It should be noted that due to its simplicity and pervasive application, distillation plays a significant role in traditional separation technology. Since 1972, surface adsorption has in some ways prevailed over the energy-dependent distillation process and has gained much momentum in the scientific community; and is a phenomenon in which a fluid (gas, liquid, or mixture) adsorbs to a solid surface and forms a chemical or physical bond. It has been developed as an efficient and fundamental approach (Foo et Hameed 2009). Separation by adsorption is, of course, more economically favored when the adsorption separation or selectivity coefficient is much higher than the relative volatility coefficient. In other words, when the relative volatility is less than about 1.25, adsorption is superior to distillation separation.

The adsorption process often takes place in a fixed bed of adsorbent on which the reformation operation is performed periodically. A conventional system consists of two parallel substrates, one in which it is in the state of adsorption and the other in which it is being reformed. In large industrial units, the use of three substrates is constant. Thus, two beds are always being adsorbed, and one bed is being restored. At low temperatures, adsorption is typically accomplished through intermolecular forces rather than the formation of new chemical bonds. This is why it is referred to as physical adsorption. However, activation energy is available to form or break chemical bonds at temperatures above 200°C. As a result, this mechanism is known as chemical adsorption. Physical adsorption is primarily accomplished through van der Waals and electrostatic forces between adsorbed molecules and the atoms that comprise the adsorbent surface.

The levels of porous adsorbent are often unpredictable, and the bond energies vary significantly from one active site to another. Of course, in molecular sieves, which are examples of surfaces with high uniformity, the connection energy is almost constant. Adsorbent surfaces in internal channels or cavities have microcrystalline structures. Adsorbents are usually synthetic or natural materials with amorphous or microcrystalline structures. Adsorbents that are commonly used include activated carbon, activated alumina, silica gel, bentonite, and lignite (Tchobanoglous et al. 2003).

2.4.2 Difference between physical and chemical adsorption

In the adsorption process, a fluid can penetrate the pores of the adsorbent and come in contact with its large surface area. This mechanism in adsorption is complex, and so far, many theories have been proposed to describe the adsorption action. Physical adsorption mechanisms in which the material is adsorbed on the adsorbent surface and chemical adsorption in which the substance is absorbed by the adsorbent through a chemical reaction are the main adsorption mechanism. In the case of

adsorption, it is preferable to distinguish between physical adsorption, which is primarily related to weak intermolecular forces, and chemical adsorption, which is primarily related to the formation of chemical bonds between the adsorbent and the adsorbent surface (see Table 7).

Table 7. The general cases through which we distinguish physical adsorption from chemical

Physical adsorption	**Chemical adsorption**
Low heat adsorption	High heat adsorption
None specify	High specify
Single-layer or multilayer	Just single layer
Decomposition of adsorbed parts does not occur	Corrosion of adsorbed components may occur
Only in a small and specified range of temperatures	In a wide range of temperatures is possible
Fast and reversible	It may be slow and irreversible
We do not have electron transfer, although polarization of	Electron transfer leads to the formation of a bond between the adsorbate and the surface

Adsorption is mainly due to Van der Waals forces and intermolecular forces; thus, almost all separation processes are related to physical adsorption, so we focus on them. Estimating the adsorption capacity with adsorbent dynamics is necessary to have information on the adsorption equilibrium. Adsorption equilibrium is the essential property of adsorption action, which is investigated to determine the amount of adsorbed material under a series of known concentration and temperature conditions and the rate of particular adsorption when two or more adsorbents are present. There are many theoretical and experimental methods for determining lateral equilibrium, which in some cases are not suitable for predicting adsorption isotherms under different operating conditions. The Schematic structure of the physical and chemical adsorption is shown in Figure 6.

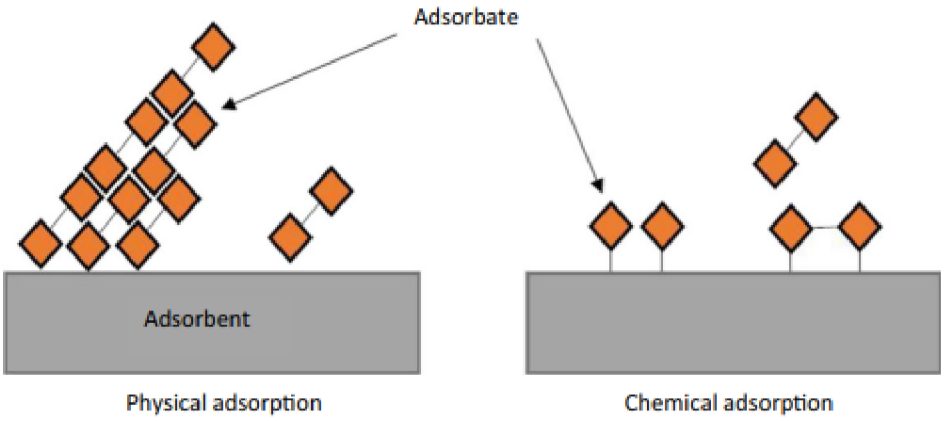

Fig.6. Schematic structure of the physical and chemical adsorption (Omar et al. 2019).

2.5 Adsorption isotherms

Isothermal models are used to analyze adsorption data in order to better understand the mechanism of adsorption on the adsorbent surface. At a constant temperature, these models express the balance of adsorbed ions (Hao et al. 2010). The equilibrium relationship between the adsorbed contaminant per unit mass of adsorbent and the residual equilibrium concentration of the solution at a constant temperature is expressed by the adsorption isotherm. Researchers have studied the adsorption isotherm model using a variety of equations.

Well-known models of these isotherms are the Langmuir and Freundlich models, whose linear equations are in the form of relations (1) and (2):

$$Lnq = Lnk_j + \frac{1}{n}.Lnn.C \qquad \text{Langmuir} \qquad (1)$$

$$\frac{1}{q} = \frac{1}{q_{\max}} + \frac{1}{bq_{\max}}.\frac{1}{c} \qquad \text{Freundlich} \qquad (2)$$

Where, C is concentration (mg/l), q is adsorbent adsorption capacity (mg/g), q_{max} is maximum adsorption capacity (mg/g), b is Langmuir equation constant, n is Freundlich equilibrium constant, k_f is Freundlich isotherm constant.

The Langmuir and Freundlich isotherms are used to describe the equilibrium adsorption established between metal ions remaining in solution (C) at constant

temperature (Wei et al. 2013). In the Langmuir model, it is reported that the adsorption of metal ions occurs on a homogeneous surface in a monolayer. In contrast, adsorption occurs on a heterogeneous surface with unequal energy (Deveci et Kar 2013).

2.5.1 Adsorption complexation models

2.5.1.1 Elovich model

The Elovich equation is suitable for describing systems with heterogeneous adsorption surfaces, especially gas adsorption on solid surfaces (Xin et al. 2012). In reactions involving the chemical adsorption of the adsorbent on a solid surface and occurring without desorption, due to the fact that the surface coating increases, the adsorption rate decreases with time, which is one of the effective models to describe the chemical adsorption to the relationship form (3) is presented:

$$\frac{dqt}{dt} = a.\exp(-bqt) \qquad (3)$$

Where, *q* is the amount adsorbed ion at time t is in terms of (mg/g), *a* is initial adsorption rate (mg/g.min), *b* is and represents the rate of chemical adsorption and constant *b* adsorbent (g/mg) during each experiment, which Related to surface coating. The value of the initial adsorption rate parameter (*a*) increases with increasing initial solution concentration. If parameter *b* is related to the area of the surface coating, then the increase in the concentration of the solution to reach the adsorbent surface for the contaminant decreases. Increasing the amount of adsorbent also increases the surface accessibility for the adsorbent (Günay et al. 2007).

2.5.1.2 Pseudo-first-order model

This equation is known as the Lagergren equation and determines the adsorption rate based on the adsorption capacity, which is a relation (4):

$$\frac{dq_t}{qt} = k_1.\exp(q_e - q_t) \qquad (4)$$

Where, q_e and q_t are the adsorption capacity at the equilibrium point and at time *t*, respectively, in terms of (mg/g), k_1 is the velocity constant of the equation (1/min), which is the linear form of the equation in the form of a relation (5) (Hao et al. 2010):

$$\log(q_e - q_t) = \log(q_e) - \frac{k_1}{2.303}t \quad (5)$$

2.5.1.3 Pseudo-second-order model

The pseudo-second-order kinetic model has a high ability to describe the mechanism of adsorption of contaminants on adsorbents with active sites. This model is based on the adsorption capacity of solid phases. Unlike other models, it predicts the adsorption behavior of the whole process, which is presented as a relation (6):

$$\frac{d(q)_t}{d_t} = k_2(q_e - q_t)^2 \quad (6)$$

where, q_e and q_t are, respectively, with the adsorption capacity at the equilibrium point and at time *t* in terms (mg/g), k_2 is constant in the velocity of the equation in terms (g/mg.min).

The linear form of the equation can be expressed as (7) (Hao et al. 2010):

$$\frac{t}{qt} = \frac{1}{k_2 q_e^2} + \frac{t}{q_e} \quad (7)$$

2.5.1.4 Thomas model

Maximum adsorption capacity is required at levels, and the Thomas model was used to accomplish this goal. The data obtained from the column are obtained in continuous mode to calculate the constant adsorption rate as well as the maximum concentration of the adsorption capacity of the column using the kinetic model. The Thomas model is one of the most common and widely used methods in a columnar operation. The Thomas model for an adsorption column is presented in the form (8):

$$\frac{c_t}{c_0} = \frac{1}{1+\exp(k_{th}q_e x / Q - k_{th}c_0 t)} \quad (8)$$

Where, the kinetic coefficient k_{th}, and the adsorption capacity q_t can be detected from a design $\frac{c_t}{c_0}$ versus t for the given velocity using nonlinear regression analysis.

2.5.1.5 Adams-Bohart model

This model assumes that the adsorption rate is relative to the residual adsorbent capacity and concentration of adsorption species. This equation can be obtained from scheme c versus t at a given bed height and flow velocity and is expressed as (9):

$$\frac{c_t}{c_0} = \exp(k_{AB}c_0 t - k_{AB}N_0 \frac{z}{u_0}) \quad (9)$$

where, Z is the column height, N_0 is the maximum Adams-Bohart absorption capacity, K_{AB} is the Adams-Bohart kinetic constant, and U_0 is the longitudinal linear velocity.

2.5.1.6 Yoon-Nelson model

Not only is this model less complex than other models, but it does not require any detailed data regarding the characteristics of the adsorbent, the type of surface adsorbent, and the physical components of the adsorption bed.

This approach involves the concentration of (c) versus sampling time (t) according to the following equation that the K_{YN} and τ parameters can be obtained using the nonlinear regression method according to equation (10):

$$\frac{c_t}{c_0 - c_t} = \exp(k_{YN}t - \tau k_{YN}) \quad (10)$$

2.5.1.7 BDST model

This model is used to predict the relationship between bed height and measurement time (t) for process concentration and adsorption parameters. The BDST model assumes that the adsorption rate is controlled by the surface reaction between adsorption and capacity using the adsorbent.

The breaking time values obtained for the various bed heights are introduced in this model. The linear relationship between the bed height and the measurement time is expressed by Equation (11):

$$t = \frac{N_0}{c_0 u_0} z - \frac{1}{k_a c_0} . \ln\left(\frac{c_0}{c_t} - 1\right) \quad (11)$$

In this scheme, *t* versus *Z* must obtain a straight line, where *U* and *k* are the adsorption capacitance and the velocity constant, respectively (Jossens et Prausnitz 1978).

2.5.2 Adsorption measurement

Adsorption of Cd is one of the essential chemical processes in the soil that affects its behavior in soil and water and ultimately controls its mobility. In several studies to determine the sorption/desorption of Cd in the soil environment, X-ray spectroscopy (XS) has been used to provide information at the molecular level. The XS technique can describe adsorption reactions, and this information can significantly enhance our current knowledge of Cd chemical reactions in the soil (Hayes et al. 1987; Chisholm-Brause et al. 1990; Scheidegger et al. 1996; Gräfe et al. 2007; Xinxin et al. 2021). Two of the most important and widely used XS techniques are X-ray photoelectron spectroscopy and X-ray absorption spectroscopy, which are briefly described below.

- **X-ray photoelectron spectroscopy (XPS)** is a surface science technique that measures the experimental formula, element composition, electronic state, and chemical form of a substance surface elements, as well as the bond states of the details (Mather 2009). The XPS is a simple process; in this way, the electrons inside a sample absorb photons with specific energy and then leave the sample. Kinetic energy examination of electrons discharged from the surface gives us information about atoms on the surface (Engelhard et al. 2017); because the

electron configuration of the atom changes with the change of chemical bonds. The XPS stands out in popularity, versatility, and functionality compared to many other techniques (Engelhard et al. 2017); XPS is a robust measurement approach because it shows what elements are present and what other factors they are bonded to. The method can be used inline profiling of the elemental composition across the surface or in-depth profiling when paired with ion-beam etching (Neville et al. 2007).

X-ray absorption spectroscopy (XAS) is an approach that provides a measurement of the elemental and chemical structure of a sample due to its X-ray absorption properties. The XAS technique requires a high-power X-ray that can be adjusted over a wide range of energies and, therefore, must be performed using a synchrotron radiation source (Holbrook et al. 2015). The XAS is especially useful for studying metal oxides, as each has a specific set of adsorption edges, and XAS is sensitive to the electrons binding energies in the atom nucleus; in fact, XAS the X-ray absorption coefficient measures a substance as a function of energy (Johnston 2012). The XAS consists of two primary structures: extended X-ray absorption fine structure (EXAFS) and X-ray absorption near edge structure (XANES).

2.6 Adsorbents

2.6.1 Introduction:

Soil is a dynamic system that can cycle many organic and inorganic substances that have externally entered the soil system, such as pollutants, and can be attenuated by adsorption. Half of the common soil type is solid in soil minerals and has a relatively simple chemical bound. Numerous elements are present within naturally occurring soils due to various pedogenetic processes, such as primary weathering, biological deposition, or climatic influence. Oxygen is the most abundant present element in the soil and the

second abundant element is Si which is critical for the structure of silicate minerals in the soil. Silicates, carbonates, sulfides, and oxides are widespread minerals primary groups in soil with several species (Strawn et al. 2020). Among many materials, metal oxides are promising for immobalizing heavy metals in the environment, especially in the soil phase, due to their easy transport, stability, and low cost (Hua et al. 2012; Arora 2018). Also among metal oxides are iron oxides (Benjamin et Leckie 1981; Kyzas et al. 2015; Komárek et al. 2018; Shi et al. 2021; Leiva et al. 2022) and manganese oxides are often used due to their high specific surface area (Wasylenki et al. 2014; Ratie et al. 2021; Wang et al. 2022).

Iron oxides are found in abundance in nature and are of great importance in some industries (Vu et al. 2013). The adsorption of Cd on iron (oxyhydr) oxides is related to the nature and structure of minerals (Fernandes et Baeyens 2019). Iron oxides are usually formed as high-specific surfaces secondary minerals, such as goethite and ferrihydrite, and can contain large amounts of heavy metals (Guo et Barnard 2013; Li et Kaplan 2012; Peacock et Sherman 2004; Shi et al. 2021). Like iron oxides, manganese oxides play an important role in earth science. As one of the main components, manganese oxides significantly impact soil properties. Although there are different types of manganese oxides, such as, MnO, MnO_2, Mn_2O_3, and Mn_3O_4, they are primarily found in the form of MnO and MnO_2 in the environment (Miller et al. 2021). When manganese oxides in the environment (e.g., manganites and birnessite) are combined with the structure of heavy metals such as Cd, the stabilization results are auspicious. Regarding, iron oxides and manganese oxides are introduced in detail in the following subchapters.

2.6.2 Oxides of Mn

Manganese oxides have several oxidation states, and various crystalline structures of Mn (II, III, IV) in which they can be observed in the environment (Ettler et al. 2014).

Manganese oxyhydroxides can be found in most types of soils and sediments all around the world (Michalkova et al. 2016). Manganese oxides have been observed in several natural forms, such as manganese nodules, layers in sediments, hydrothermal alteration products, and rock polish forms. In addition to the mentioned natural forms, MnO_2 can be found in acid-mine drainage polluted streams. Manganese dioxide prevails in different crystalline structures, such as hollandite, pyrolusite, birnessite, akhtenskite. They appear as a coating on the particles surface area, and they have been controlling the share of metals in soil and soil solution (Michalkova et al. 2016; Post 1999; Strawn et al. 2015). Manganese oxide has been observed in the marine sediments, rhodochrosite formed in organisms as a result of biological activity and redox reaction of Mn (Ettler et al. 2014). Manganese oxides have been confirmed to have a high ability for immobilization of divalent metals and metalloids such as, Pb(II), Cd(II) and, Cu(II) (Trakal et al. 2018; Puppa et al. 2013).

Manganese oxides were discovered to be a strong adsorbents for metals and metalloids; however, their reactivity and stability should be considered when used as a decontamination method in the soils that are contaminated with metals or metalloids. (Ettler et al. 2014). Manganese oxides have been used for water and soil treatment, and it can influence the speciation and mobility of metal and metalloids even at low concentrations (Ouředníček et al. 2019). Some of the most common natural manganese oxides that can be used to adsorb Cd are introduced in the following subchapters.

2.6.2.1 Birnessite

Birnessite mineral was discovered in Scotland in 1956 and is a natural state. Birnessite is the most abundantly occurring manganese oxide mineral and one of the most abundant oxide minerals in general (Sposito 2008). Birnessite forms by precipitation in water bodies with many base cations, such as groundwater or lakes; the birnessite minerals have a biogenic source (Strawn et al. 2020). Birnessite minerals can be found

in the soil, coating the other particles surfaces. Many empty cationic sites express a negative net surface charge within their mineral structure, allowing the mineral phase to adsorb various cations (Post 1999). According to studies, there are structural issues associated with the mineral birnessite, and these parts are often rapidly occupied via isomorphic substitution; however, in the case of adsorption processes, stronger cations may occupy these sites (Strawn et al. 2020). Naturally occurring birnessite often has a poorly crystalline structure and is highly fine-grained (Post 1999; Sposito 2008). Initially, it was impossible to analyze natural samples; instead, birnessite 'like' phases had to be chemically synthesized to be analyzed (Post 1999).

Birnessite holds a layered structure and has been applied as an adsorbent (Dawadi et al. 2020). The birnessite physicochemical properties depend on the specific surface area and average oxidation number, which highly depends on the synthesis condition. During the synthesis, by increasing the aging time, the purer birnessite can be obtained. According to the XRD (X-Ray Diffraction) studies, birnessite shows several crystalline properties associated with the composition and method used for synthesis (Min et Kim 2020). To obtain pure minerals of birnessite, fundamental synthesis methods are considered, such as oxidation of Mn_2^+, redox reactions between Mn_2^+ and MnO_4^-, and reduction of MnO_4^-. According to Post (1999), the actual structure of natural Birnessite can be estimated until improved XRD and XANES (X-ray Adsorption Near Edge Structures) techniques have been employed. This mineral has a few features that make it a good choice for studying mineral adsorbent potentials. Strong electronegative metallic cations are easily bound within the structure cationic gaps, keeping them biologically inaccessible. Finally, this mineral poor crystalline structure allows for a more uneven surface charge, which increases the chance of available active sites for metallic ions from the solution (Sposito 2008).

2.6.2.2 Manganites

Manganites were discovered for the first time in 1950. Due to the manganese ion, which is a crucial ingredient of the compounds of its mixed-valence state, the material is named manganite (Bassani et al. 2005). In contrast to the usual ferromagnetics, the transition of manganites to a ferromagnetic state is followed by an extreme increase in conductivity. Such transition from an isolator to a metallic and magnetic state is a notable fundamental feature of these materials. Another essential property is the colossal magnetoresistance effect, one can observe a significant change in the resistance in the existence of a moderate applied magnetic field (Kumar et al. 2013; Spurgeon et Chambers 2017; Bhongale et al. 2018).

2.6.3 Oxides of Fe

The most abundant metallic oxides in the soil are the oxides of Fe. Usually, the Fe is released to the soil solution by weathering of silicates and sulfide minerals (Liu et Huang 2005). The oxidation of the Fe(II) depends not only on the solution but also on the iron speciation in the solution (Koretsky 2000). Oxides of Fe include lepidocrocite, maghemite, hematite, goethite, and ferrihydrite (Komárek et al. 2018). Magnetite (Fe_3O_4), hematite (α-Fe_2O_3), and maghemite (γ-Fe_2O_3) are the most known Fe oxides. The citric acid released from the plants roots has a significant effect on the Fe oxides formation and alters their surface properties such as their structure, chemical composition, the effect on the specific surface area, surface porosity, and surface charge (Liu et Huang 2005). Maghemite (γ-Fe2O3) has shown cubic spinel structure, hematite (α-Fe2O3), on the other hand, has a corundum structure. Hematite is the most stable form of Fe oxide and the weakest ferromagnetic one. Magnetite and maghemite-based Fe nanoparticles have excellent adsorption capacity, recyclability, high mobility, cost-efficiency, stability,

and easy separation to use on an industrial scale, for example, in wastewater treatment (Abdullah et al. 2019).

Several methods have been suggested to synthesize Fe oxide, such as chemical co-precipitation, hydrothermal route, sol-gel, and thermal decomposition (Abdullah et al. 2019). Co-precipitation is a simple, effective, and cheap method to synthesize Fe oxide on a large scale. The co-precipitation method has been conducted by mixing ferric and ferrous with the same molar ratio at room temperature or elevated temperature. During the procedure, the nano-particles shape and size can be controlled by varying the type of the salts, the temperature, ferric and/or ferrous ions ratio, the pH, ionic strength of the media, or other reaction parameters set in the procedure such as stirring rate, and dropping speed of the basic (alkaline) solution. Several studies suggest using the Fe^{3+} and Fe^{2+} charged of Fe to produce nanoparticles of Fe oxide by the co-precipitation; for example, ferrous chloride, ferrous sulfate, and ferrous ammonium sulfate can be used as a source of Fe^{2+} cation. While ferrous chloride, ferrous sulfate, and ferrous ammonium sulfate can be used as a source of Fe^{2+} cation, ferric chloride and ammonium ferric sulfate have been used as Fe^{3+} sources (Abdullah et al. 2019).

Iron oxides reactive functional group -OH and $–OH_2$ play a significant role in controlling the metals mobility and bioavailability (Liu et Huang 2005). Iron oxide and oxyhydroxide affect the immobilization of contaminants in soil solution through reactions such as precipitation, change of the speciation, and co-precipitation (Vítková et al. 2018). According to the studies, the increase in the pH of the soil in the presence of Fe oxyhydroxide mostly depends on the initial pH of the soil and any present oxidants such as O_2, NO_3^- SO_4^{2-}, H_2O, and its microbial composition (Vítková et al. 2018). On the other hand, the potential toxicity of Fe amendment in the soil is a controversial objective in the studies. Iron oxyhydroxide application can be toxic to living organisms (Vítková et al. 2018).

In general, iron oxides and hydroxides are efficient adsorbents, but goethite and ferrihydrite, in particular, have inherent structures that can take on a variety of shapes. The metastable ferrihydrite minerals may change into more stable goethite in oxygenated aquatic conditions; ferrihydrite reduction can significantly speed up the adsorption of divalent candidate heavy metals, which can be coupled with newly created goethite. According to Cornell and Schwertmann (2003), goethite and ferrihydrite are both sensitive to high rates of isomorphic substitution and are frequently found with impurities comprising calcium oxides or manganese oxide.Because of their disordered structure, high charge density, and higher than usual surface areas, iron-based minerals are adequate adsorbents of transitional or heavy metals. Some of the most necessary natural iron oxides that can be used to adsorb Cd are introduced in the following subchapters.

2.6.3.1 Goethite

Goethite is the most naturally abundant iron oxide mineral in the temperate regions and mostly in humid areas on the earth surface, and it is the byproduct of the secondary weathering of the magnetite, pyrite, and siderite (Cornell et Schwertmann 2003). The chemical formula of goethite is FeO(OH), FeO_2H, or $Fe_2O_3.H_2O$. In terms of chemical composition, it contains 89.9% of Fe_2O_3 and 10.1% of water. The iron content of this mineral is 62.9%. Goethite has a crystalline shape and a dark brown or black color. This mineral typically has magnetic properties. Goethite is mostly found in nature along with metal sulfides and carbonates. Goethite deposits are sometimes composed of oxidation of siderite and silicates. Due to heat, goethite loses its crystallization water and becomes entirely porous for particles that have higher regenerative properties (John 2021). The iron ions in goethite are chemically improperly coordinated on the mineral edge structures, leading to a net charge imbalance that allows hydrogen (H^+) or hydroxide (OH^-) complexation, resulting in different functional, high affinity (Strawn et al. 2020).

2.6.3.2 Ferrihydrite

Ferrihydrite is a naturally disordered mineral with many other natural variants (Cornell et Schwertmann 2003). The formation of ferrihydrite happens in the acidic soil with excess organic matter and microorganisms, and it is considered one of the most reactive types of iron hydroxides phase (Vodyanitskii 2016; Cornell et Schwertmann 2003). Ferrihydrite is the predecessor for most iron oxides in soil, and it later transforms to more stable minerals such as goethite. Ferrihydrite ($(Fe^{3+}•10O•14(OH)_2)$) forms a considerable proportion of soils, especially soils formed under low-temperature, moist conditions. The complex surface and the high reactivity cause ferrihydrite to become a powerful adsorbent of metals and organic species in natural waters (John 2021). Due to the specific requirements of formation and high reactivity of the mineral, ferrihydrite is extremely rare to find in pure mineral form; ferrihydrite found in the environment is often combined with other molecules or ions. Ferrihydrite is found in nanoparticles, and the mineral disorganized structure allows for the complexation of most divalent cations. The ephemeral nature of ferrihydrite stems from its brief existence as a pure mineral; prior to the development of amorphous absorption spectroscopy (XAS), little was known about the appropriate crystalline structure (Vodyanitskii 2016).

3 Experimental part

3.1 Methodology

3.1.1 Sorbent characterization

To evaluate the Cd isotopic fractionation during adsorption processes on environmentally-relevant matrices, two Fe (oxy)hydroxides, ferrihydrite and goethite, were chosen as representatives of amorphous/slightly crystalline and crystalline Fe oxides present in soils, wetlands, forming coatings on roots, etc. Ferrihydrite (namely a 2-Line Ferrihydrite) was prepared by precipitation according to the method by

Schwertmann and Cornell (2003). In short, 40 g of $Fe(NO_3)•9H_2O$ was dissolved in 500 mL of deionized water. Subsequently, 330 mL of 1 M KOH were added under vigorous stirring until the final pH between 7 and 8 was reached. Originated reddish precipitates were separated using filter paper, washed thoroughly five times with deionized water, and dried at 35°C. Goethite was purchased in the form of commercial product Bayoxide® E F 20 (Lanxess). The mineralogical composition of both phases was confirmed using X-ray diffraction analysis (Bruker D2 Phaser with an LYNXEYE XE detector) (Fig.7). The specific surface area of both materials was determined using the Brunauer-Emmett-Teller (BET) method (ASAP 2050 instrument, Micrometrics Instrument Corporation, USA) and equaled to 304 m^2/g and 118 m^2/g for ferrihydrite and goethite, respectively.

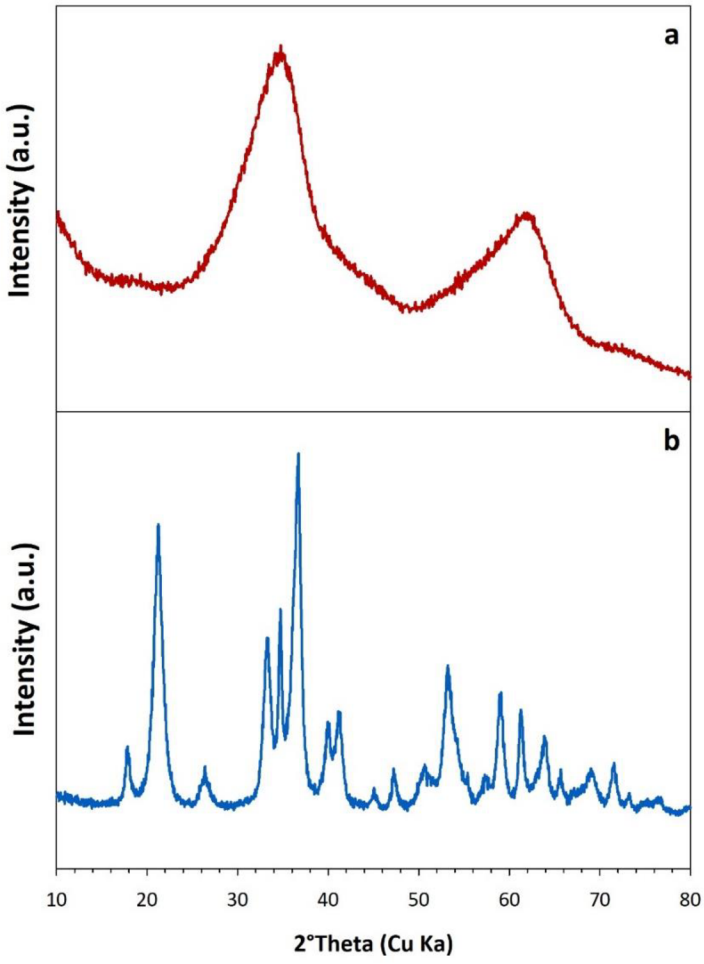

Fig.7. X-ray diffraction patterns of ferrihydrite (a) and goethite (b) used in the study. The diffractograms are in accordance with those of ferrihydrite (Cornell and Schwertmann 2003), and goethite (ICOD 00-029-0713).

3.1.2 Adsorption experiments

To investigate the Cd sorption and corresponding isotopic fractionation during the complexation with both ferrihydrite and goethite, a set of adsorption experiments was performed. Firstly, adsorption kinetics and related Cd isotopic fractionations were determined, as these data will later serve as a background for following determination of adsorption edges.

All the adsorption experiments (both kinetics and adsorption edges) were performed under the inert (N_2) atmosphere to avoid the carbonates precipitation. To reach these conditions, deionized water for the experimental solutions was over-boiled and cooled down under constant purging with N_2. The experimental suspensions contained 4 g L^{-1} of ferrihydrite or goethite and the Cd concentration was set to 10^{-4} mol L^{-1} (Cd isotope standard NIST 3108 Cd). Kinetic experiments for both materials were performed under the ionic strength of 10^{-1} mol L^{-1} $NaNO_3$ and pH 7 (controlled by the addition of $NaOH/HNO_3$). After adding the sorbents to the experimental solutions saturated with N_2, the originated suspensions were then agitated for different time intervals up to ~200 hours. A separate test tube was used for each time interval. After reaching the target time, experimental suspensions were filtered immediately through a 0.22 µm nylon syringe filter, and the concentration of Cd in solution was determined using inductively coupled plasma optical emission spectrometry (ICP OES; 720 Series, Agilent Technologies). Based on the difference between the initial concentration of Cd in solution and its concentration after adsorption, it was possible to calculate the corresponding amount of Cd adsorbed by the ferrihydrite/goethite at each time interval. The Cd isotopic

ratios in the filtered solutions were subsequently determined using thermal ionization mass spectrometry (TIMS) – see below, chapter 3.1.3.

The data obtained from kinetic experiments (adsorption equilibrium time and isotopic equilibrium time) provided the background for the determination of adsorption edges. Here, the experimental solutions were prepared in a similar way as in the case of kinetic experiments, using 4 g L^{-1} of ferrihydrite/goethite, ionic strengths of 10^{-1}, 10^{-2} and 10^{-3} mol L^{-1} $NaNO_3$, and Cd concentration of 10^{-4} mol L^{-1} (Cd isotope standard NIST 3108 Cd). After adding the ferrihydrite/goethite to the experimental solutions, the pH was adjusted using $NaOH/HNO_3$ to be within the range of ~3 to ~10. Suspensions were left to agitate for 24 hours and after that, the final pH was measured. The samples were then centrifuged (15 mins, 7000 rpm), filtered through a 0.22 µm nylon syringe filter, and the concentration of Cd in solution was measured using ICP-OES. Due to the time range when these laboratory experiments (the year 2020) for this Diploma thesis were performed, it was not possible to finish due to the covid-19 pandemics also the Cd isotopic measurement for the solutions from adsorption edges experiments. Yet, these analyses were subsequently finished later, and the data in this thesis thus served as a basic background for following analyses, elucidating more the processes of Cd isotopic fractionation during complexation with ferrihydrite and goethite.

3.1.3 Isotopic analyses

To assess the Cd isotopic fractionation kinetics during adsorption onto both Fe oxides, the Cd isotope ratios in filtered solutions from adsorption kinetic experiments were determined using the thermal ionization mass spectrometry (TIMS, Triton, Thermo Fisher). The Cd isotopic compositions were expressed as $\delta^{114/110}Cd$, relative to the NIST SRM 3108 (Eq. 12):

$$\delta^{114/110}Cd = \left(\frac{\left(\frac{^{114}Cd}{^{110}Cd}\right)_{sample}}{\left(\frac{^{114}Cd}{^{110}Cd}\right)_{NIST\ SRM\ 3108}} - 1 \right) \times 1{,}000 \qquad (12)$$

The double-spike (DS) method was used to correct the raw isotopic measurements for potential isotopic fractionation during Cd column separation and the TIMS analysis. The DS was prepared by mixing two enriched Cd isotope spikes: ^{106}Cd (97%) and ^{116}Cd (99%) (IsoFlex, USA) at the ratio of 35% of ^{106}Cd to 65 % of ^{116}Cd. The DS was subsequently added to the samples before the Cd separation process. The natural/DS ratio was 5.6 for ^{106}Cd/^{110}Cd and 10.8 for ^{116}Cd/^{110}Cd. The $\delta^{114/110}$Cd value was measured for the international reference standards NIST SRM 3108 and BAM 1012 with the long-term external precision of ± 0.02 ‰ (2SD, n=3) and ±0.08‰ (2SD, n = 12), respectively (Ratié et al. 2021).

To prepare the samples for the TIMS measurements, it was needed first to separate the Cd using chromatographic separation. Prior to this step, the sample solutions were evaporated and transferred to the bromide form (HNO_3 (0.5M)-HBr (0.2M)). The following Cd separation was performed according to the protocol by Ratié et al. (2021) based originally on the methods of Schmitt et al. (2009a; 2009b) and Abouchami et al. (2011; 2014) (Table 8).

Table 8. The procedure of column chromatograpich Cd separation (Ratie at al. 2021)

2 mL column BioRad + 0.4 ml Resin AGI-X8 100-200 mesh

Order	Process	Step	Reagent	Volume	Time	Dose
Part I	Washing Column	1	HNO_3 (0.5M) normal pur	4 (mL)	2	2 (mL)
		2	H_2O MQ	4 (mL)	2	2 (mL)
Part II	Conditioning	1	HNO_3 (0.5M) HBr (0.2M) Ultrapur	4 (mL)	4	1 (mL)
Part III	Sample loading	1	HNO_3 (0.5M) HBr (0.2M) Ultrapur	2 (mL)	4	0.5 (mL)
Part IV	Matrix elution	1	HNO_3 (0.5M) HBr (0.2M) Ultrapur	2 (mL)	4	0.5 (mL)
		2	HNO_3 (0.45M) HBr (0.)3M) Ultrapur	3 (mL)	3	1 (mL)
Part V	HBr removing	1	HNO_3 (0.25M) Ultrapur	100 (mL)	1	100 (µL)
Part VI	Cd recovery	1	HNO_3 (0.25M) Ultrapur	6 (mL)	6	1 (mL)

Recovered Cd solutions were evaporated on a hot plate (110 °C-120 °C) until the last drop. After cooling down, an activator consisting of 50 µL of H_3PO_4 0.1 N and 100 µL of silica gel per 500 ng of Cd in sample was added. The mixture was then evaporated to the dryness and 15 µL of HNO_3 (2%, v/v) were added. Samples were subsequntly ultrasonicated for better homogenization and loaded stepwise onto an outgassed single Re filament. Cadmium isotope ratios were measured by TIMS using a Triton (Thermo Fisher) instrument.

4 Results

4.1 Adsorption and isotopic kinetics of Cd onto ferrihydrite and goethite

The kinetic evolution of the fractionation of Cd sorbed at pH = 7, [Cd] = 10^{-4} mol L^{-1}, and [$NaNO_3$] = 10^{-1} mol L^{-1} for both ferrihydrite and goethite is shown in Figure 8.

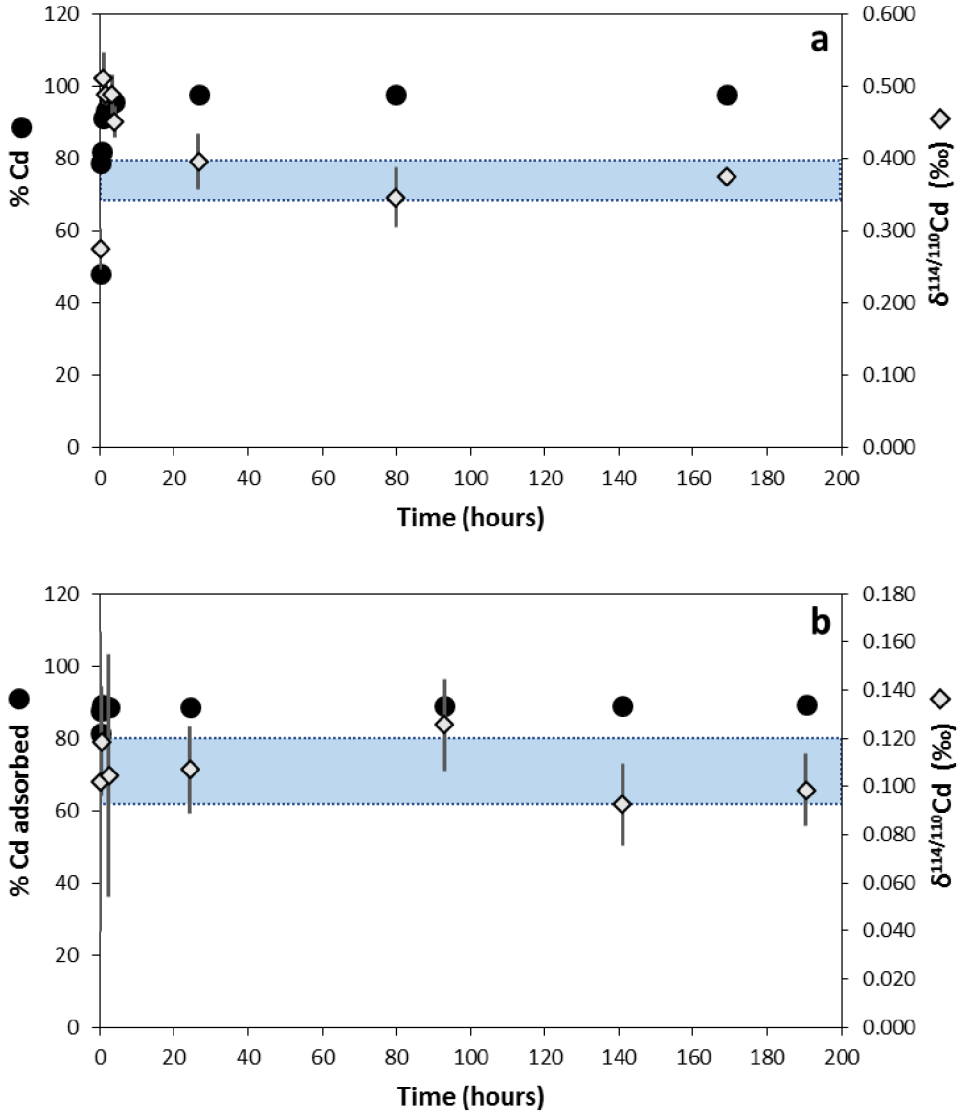

Fig.8. Evolution of the proportion of adsorbed Cd in time and its isotopic fractionation during adsorption onto ferrihydrite (a) and goethite (b).

As shown in Figure 8, The blue shaded areas depict the mean of the $\delta^{114/112}$Cd values for all time intervals ≥ 24 hours ± the corresponding standard deviation: i.e., 0.372 ± 0.025‰ for ferrihydrite and 0.106 ± 0.014‰ for goethite. Cadmium adsorption on the two studied materials was generally very high, with 79% and 87% of Cd adsorbed onto ferrihydrite and goethite, respectively, after only 15 minutes (Fig. 8). In the case of

goethite, the adsorption equilibrium was reached by adsorption 89% of total Cd after 30 minutes, but adsorption onto ferrihydrite increased progressively over 24 hours to 98% of total Cd adsorbed. Isotopic kinetics of Cd were also examined as part of the kinetic experiment, as the time required to reach isotopic equilibrium can differ significantly from the time required to reach adsorption equilibrium (Bryan et al. 2015). Isotopic kinetics onto goethite (Fig. 8b) was relatively quick in our case, reaching a plateau after the first 30 minutes, similar to adsorption equilibrium. In the case of ferrihydrite (Fig. 8a), there is a brief kinetic effect during the first 5 hours, but the isotopic equilibrium is reached after 24 hours. The observed results indicate that a 24-hours equilibration time is sufficient to achieve both adsorption and kinetic equilibria. As a result, this equilibration time was used in the following experiments to investigate the pH dependency of Cd sorption and isotopic fractionation.

4.2 Adsorption edges of Cd onto ferrihydrite and goethite

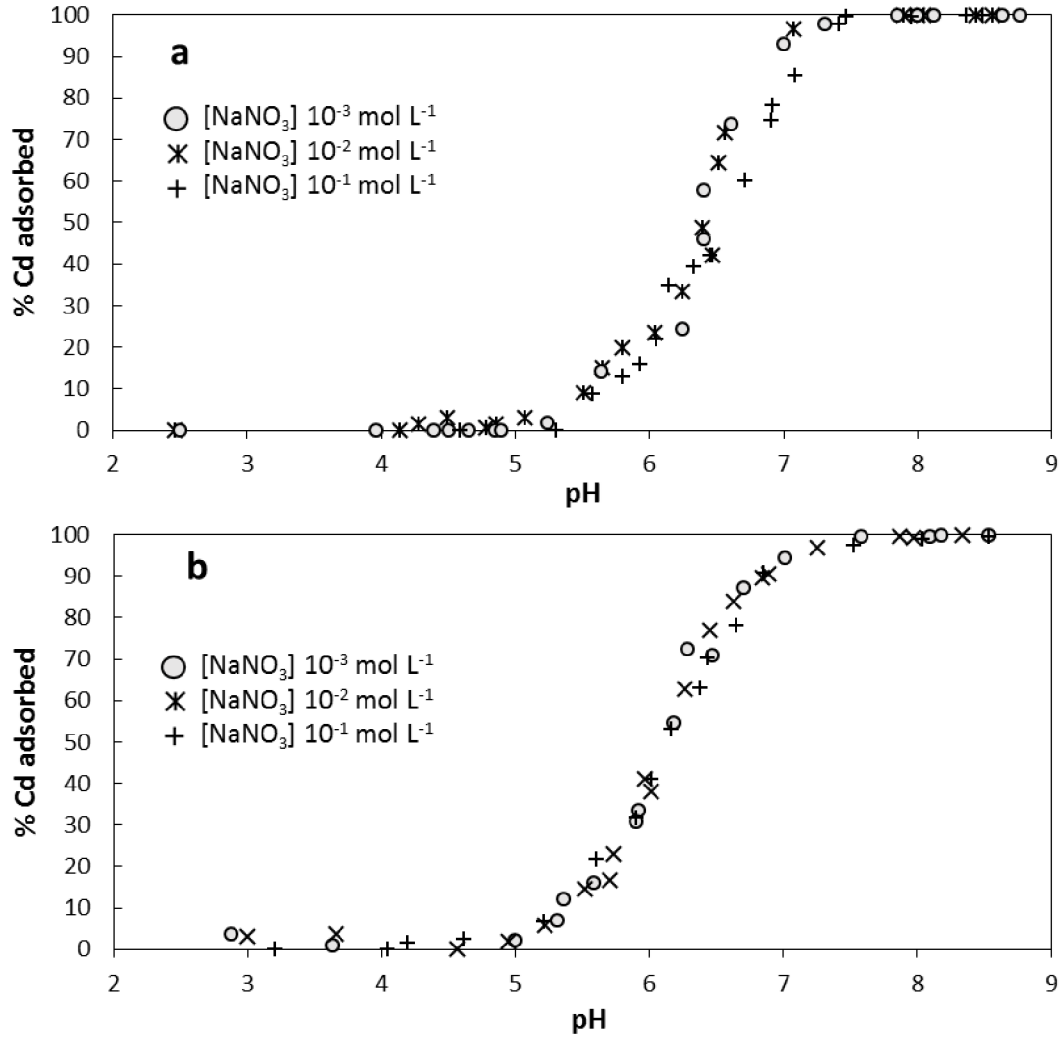

Fig.9. Adsorption edges of Cd during adsorption onto ferrihydrite (a) and goethite (b).

Based on figure 9, adsorption edges for Cd sorption onto ferrihydrite have been built at pH levels ranging from 3 to 10 with ionic strengths of 0.001, 0.01, and 0.1 M of $NaNO_3$ as the background electrolyte. The range of significant adsorption (30%+) of Cd on ferrihydrite occurred at pH 6, with maximum adsorption across all three ionic strengths occurring at pH 7.5. The effects of ionic strength on ferrihydrite adsorption were difficult to detect with the graphical visualization alone (Fig.10); however, it was easier to see that there were minute differences when combined with the data. In some cases, samples

extracted from the lower pH range of the 0.001M samples revealed traces of contamination, resulting in negative sorption. In terms of Cd adsorbance, ferrihydrite has a narrow pH range (6.5 to 8.7). (30% to 100%).

Adsorption edges for Cd sorption onto goethite were built at pH levels ranging from 3 to 10 with ionic strengths of 0.1, 0.01, and 0.001M, $NaNO_3$ as the background electrolyte. The pH range of significant adsorption (40%+) of Cd on goethite was 6 to 7.5, with maximum adsorption across all three ionic strengths at pH 8. All observed data from each ionic strength showed similar results: from lowest to highest ionic strength, each sample reached maximum adsorption capacity at pH values ranging from 7 to 8.5. In Cd adsorption (40%+), Goethite had a narrow pH range (6 to 7.5).

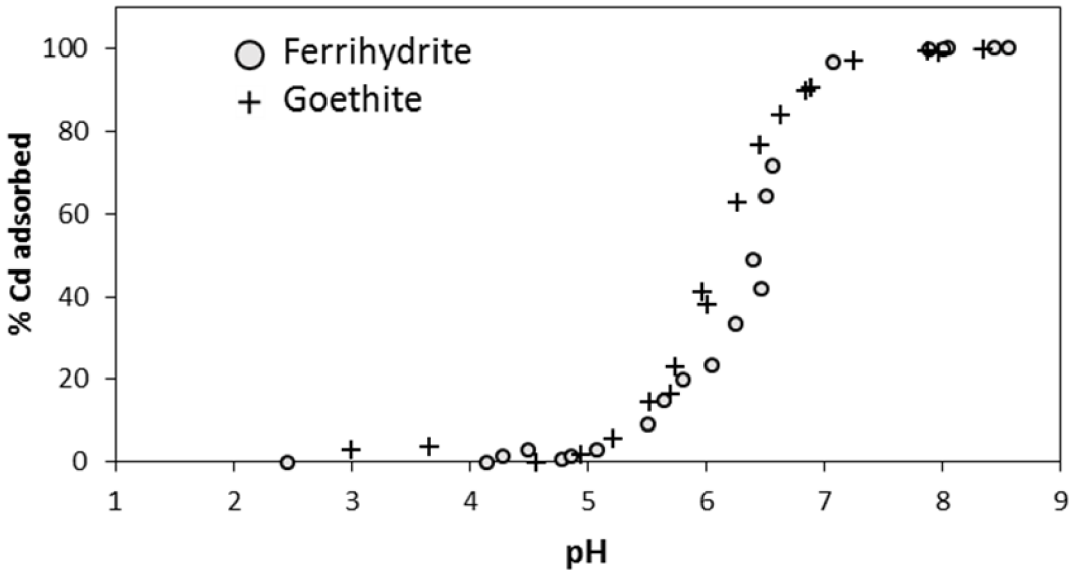

Fig.10. Comparison of adsorption edges of Cd during adsorption onto ferrihydrite and goethite.

A shown in figure 9, the adsorption edges at three different ionic strengths (10^{-1} mol L^{-1}, 10^{-2} mol L^{-1}, and 10^{-3} mol L^{-1}, $NaNO_3$) were created to evaluate the isotopic fractionation of Cd during adsorption onto ferrihydrite and goethite. Because ionic

strength had such a minor (or non-existent) effect, the 10^{-2} mol L^{-1} ionic strength data were used to compare the two directly examined phases (Fig.10). For both phases, the proportion of adsorbed Cd increased dramatically from pH 5 to roughly pH 7.5, with the highest sorption occurring around pH 7.5. However, the form of the adsorption edge differed slightly between ferrihydrite and goethite. For example, at pH 6, around 30% of Cd was adsorbed onto ferrihydrite, while approximately 40% was adsorbed onto goethite. At pH 6.5, nearly half of the Cd was adsorbed to ferrihydrite, while the other half was adsorbed to goethite. The our result of adsorption edges of Cd during adsorption onto ferrihydrite and goethite at pH = 2-10, [Cd] = 10^{-4} mol L^{-1}, [$NaNO_3$] = 10^{-1} mol L^{-1}, 10^{-2} mol L^{-1}, 10^{-3} mol L^{-1} is shown in figure 15.

5 Discussion

5.1 Effect of solution pH on adsorption

The adsorption of cadmium on goethite and ferrihydrite is pH-dependent, as it has been illustrated in figure 9 and 10. Experiments were carried out at different pH values ranging from 3 to 10, with an initial metallic ion concentration of 10^{-4} mol L^{-1}, to determine the optimum pH for Cd^{2+} adsorption on goethite and ferrihydrite. The results (Figure 10) showed that pH significantly affected Cd^{2+} adsorption on goethite and ferrihydrite. The removal efficiency increased with increasing solution pH until reaching a plateau at pH ~7. The removal efficiency of Cd^{2+} in goethite and ferrihydrite increased to ~98 percent with increasing pH from 6.5 and then remained nearly constant when getting a pH of 7.3 and above.

According to the study by Vinh et al. (2019) the surface charge of the goethite could change as in the following equilibriums:

(a) $FeOH + H^{+} \leftrightarrow FeOH^{2+}$ & (b) $FeOH \leftrightarrow FeO^{-} + H^{+,}$

the feasibility of goethite for contaminant removal was noticeably dependent on the pH of the solutions. According to the low pH, the equilibrium will be dominant, and the surface will be positively charged; at high pH, the equilibrium was dominant, and the surface was negatively charged. This means that goethite affinity for cations increased as pH increased which was confirmed by the results from our experiments (Vinh et al. 2019). Furthermore, the result of the Cd adsorption onto ferrihydrite by Yao et al. (2014) agree with the result from our experiment. At low pH, the removal of cadmium ions was inhibited by H^+ that surrounded the adsorbent surface, preventing Cd ions from approaching the adsorption sites present on the surface of ferrihydrite, and site protonation would also reduce cadmium ion adsorption. Adsorption of cadmium ions became more favorable as pH increased due to deprotonation of adsorption sites, resulting in more sites available for binding with cadmium ions (Yao et al. 2014).

The positively charged surface of minerals explains Cd^{2+} low affinity for goethite and ferrihydrite at lower pH. The surface is positively charged because the pH is lower than the pH_{pzc} (Point of Zero Charge) of goethite and ferrihydrite; the pH_{pzc} for synthesized ferrihydrite showed a range of 7-9 (Schwertmann et Fechter 1982) and the pH_{pzc} of synthesized goethite has been determined at the range of 8.1-8.2 (Appel et al. 2003). As the pH of the adsorption edge shifted upward, the repulsion interaction between Cd^{2+} and H^+ became weaker, and the surface became more charged with negatively charged functional groups (Ogata et al. 2020). Fast adsorption of Cd onto goethite and ferrihydrite from pH ~6.5 was observed due to the pH shift. This also allows metal ions to form inner-sphere complexes through chemisorption on the surface of mineral phases (Strawn et Bohn 2015). In our results, we found that the ionic strength of the solution had no effect on the adsorption of Cd on goethite and ferrihydrite (figure 9a, 9b); which can be denoted to prevailing of chemical adsorption to physical adsorption.

5.2 Adsorption and isotopic kinetics

To determine the optimum adsorption contact time, Cd^{2+} adsorption on goethite and ferrihydrite was studied for up to 200 hours at a pH range of 3-10 and an initial Cd concentration of 10^{-4} mol L^{-1}. The adsorption data revealed that removal efficiency increased until when the contact time reached equilibrium. After 24 hours of contact time, the efficiency nearly remained constant, indicating that the adsorption was saturated. Similarly, Cd(II) adsorption on goethite increased dramatically from 45% to 98% in 15 minutes, then remained nearly unchanged for the next 24 hours.

Although there is not much information about the isotopic fractionation of Cd and equilibrium of Cd, it is possible to refer to other studies and try to explain the isotope equilibrium time of Cd. Ratie et al. (2021) conducted adsorption experiments of Cd to humic acid under a variety of conditions, including different Cd concentrations (ranging from 10^{-6} to 10^{-4} mol L^{-1}), ionic strength (ranging from 10^{-3} to 10^{-1} mol L^{-1}), and pH (ranging from 4 to 6); the results of isotope fractionation and isotope kinetics suggested that the Cd isotopic composition remained constant throughout the experiment at the high ionic strength ($NaNO_3$, 10^{-1} mol L^{-1} and the Cd concentration of 10^{-4} mol L^{-1}). However, the isotopic composition quickly reached a plateau after 5 hours at pH ~4.5 at low ionic strength ($NaNO_3$, 10^{-3} mol L^{-1} and the Cd concentration of 10^{-6} mol L^{-1}). The calculated $\delta^{114/112}$Cd vlues in the solution showed range between 0.2 ± 0.02 to 0.22 ± 0.01‰, indicating the tendency of lighter Cd isotopes for complexation. However, the results from our experiment have not shown any effect of ionic strength on the adsorption and equilibrium time; also, in our experiment we reached the equilibrium in 24 hours, and in the study by Ratie et al. (2021) in the presence of humic acid the equilibrium has reached after 5 hours. Nevertheless, the tendency of the lighter isotopes for complexation can be concluded from both experiments.

However, the physiochemical behavior of Zn and Cd are similar in the environment with respect to the adsorption characteristics or their dependency on the pH; but in the fractionation of isotopes their behavior is different. Lighter isotopes of Cd tend to make the complexation and their heavier isotopes are strongly bounded in the aqueous phase, on the other hand, the heavier isotopes of Zn are founded to make the complex (Wasylenki et al. 2014; Juillot et al. 2008). The study by (Juillot et al. 2008) on the fractionation of Zn in the presence of two sorbents (ferrihydrite and goethite) has shown a considerable fractionation of Zn. The equilibrium between the adsorbed Zn and Zn in the aqueous phase has been reached after 16 hours and by comparing the adsorbed isotopes and aqueous ones after the equilibrium exibit the tendency of heavier isotopes for complexation; which contradict the result from the experiments on the Cd isotopes fractionation.

Two kinetic models have been used to investigate the kinetics of Cd adsorption onto goethite by Vinh et al. (2019); Pseudo-first-order model and Pseudo-second-order model. The values calculated from the second-order model agreed with the experimental data better than the first-order model (Vinh et al. 2019). Generally, the Cd removal by FeOx is rapid in the first few minutes, and then the adsorption gradually becomes equilibrium (Khalid et al. 2017; Shahid et al. 2017; Feng et al. 2022). A large number of active sites and a high concentration of adsorbent facilitate the initial adsorption rate while the process rate is reduced to achieve equilibrium (Wang et al. 2020; Kumar et al. 2021; Li et al. 2022; Durante-Yanez et al. 2022).

However, the initial proposal of this thesis was to determine the adsorption of Cd onto the Mn oxides and Fe oxides; due to the COVID situation, the experiment has only been conducted on the adsorption of Cd onto the goethite and ferrihydrite. Nevertheless, the Mn oxides as sorbent has been discussed in the literature review section. Considering that in corresponding conditions, according to the literature, the amount of Cd adsorption

onto MnOx is more than FeOx, moreover, the reaction rate is higher in MnOx (Rizwan et al. 2018; Zhao et al. 2018; Sharma et al. 2021; Gonzalez et al. 2022; Guérin et al. 2022). The study by Chen et al. (2014) on the adsorption of Cd onto manganese oxide/active carbon fiber has been conducted by modeling the kinetic by pseudo-first-order kinetic equation and the pseudo-second-order kinetic equation; they have been used to determine the cadmium adsorption rate constants (Chen et al. 2014). The sorption dynamics of Cd(II) to manganese oxide/active carbon fiber (MO/ACF) were studied by introducing 30 g of MO/ACF into a solution containing 200 µg/L of Cd at pH 6. According to their results, the adsorption curve reached equilibrium after 3 hours which reflect the adsorption efficiency. According to the results, the experimental data fit the pseudo-first-order adsorption kinetics equation very well. Furthermore, the rate constant from comparing the experimental results and the pseudo-first-order model is 0.9562 min^{-1}, indicating that the MO/ACF with a high specific surface area facilitates ion adsorption (Chen et al. 2014).

6 Conclusion

Environmental problems due to the entry of industrial heavy metals into the environment are increasing. Heavy metal ions are bioaccumulative in the environment and show biomagnification along the food chain, so their toxicity is a severe threat to ecological and human health. Cadmium is a non-essential heavy metal that is highly toxic in low concentrations. As a result, it is necessary to immobilize/remove it from the environment by methods such as adsorption. Among many materials, metal oxides are promising for removing Cd from the environment, especially soil, due to their easy transport, stability, and low cost. Also, among metal oxides, iron oxides and manganese oxides are often used due to their high specific surface area.

Several experiments were carried out to demonstrate the effect of pH on the adsorption of Cd to goethite and ferrihydrite at various ionic strengths of $NaNO_3$ background electrolyte (0.001M, 0.01M, 0.1M). Regarding the fractionation of Cd during thr adsorption process, as it has been illustrated in figure 8, the fractionation of Cd during the adsorption on to ferrihydrite has been higher than the adsorption onto goethite. The $\%\delta^{114/112}Cd$ (figure 8a) at the range of the fractionation of Cd in the precense of ferrihydrite ranged between 0.35‰ to 0.4‰ (blue shaded area) however the fractionation of Cd in the goethite ranged between 0.09‰ to 0.12‰. Adsorption kinetic experiments and fractionation have been performed at the same ionic strengths to determine the relationship between the amount of Cd adsorbed (percent) and time. As the adsorption edge shifts to a higher pH region, the amount of Cd adsorbed on goethite and ferrihydrite increases. Cadmium had a low affinity for goethite and ferrihydrite at lower pH. The highest amount of adsorbed Cd on goethite was found at the solution lowest ionic strength, which was thought to be due to less competition for available sites on goethite between the present cations. Meanwhile, no significant effect of solution ionic strength on adsorbed Cd on ferrihydrite was observed.

According to the results from the experiment, the adsorption has reached the equilibrium (89%) after a short time (30 minutes) for goethite, and in the case of ferrihydrite, adsorption has reached its peak (98%) after 24 hours. Isotopic kinetics onto goethite was relatively fast in our case. The results show that a 24-hour equilibration time is sufficient to achieve adsorption and kinetic equilibrium. Cadmium adsorption was generally very high on the two materials, with 79% and 87% of Cd adsorbed onto ferrihydrite and goethite after 15 minutes, respectively. Result from the adsorption edges in different ionic strength has not shown significant difference and comparison between the adsorption edges of the two sorbent illustrate a minor shift in the adsorption rate of goethite.

7 References

Abdullah, N. H., Shameli, K., Abdullah, E. C., & Abdullah, L. C. (2019). Solid matrices for fabrication of magnetic iron oxide nanocomposites: Synthesis, properties, and application for the adsorption of heavy metal ions and dyes. *Composites Part B: Engineering*, *162*, 538–568. https://doi.org/10.1016/j.compositesb.2018.12.075

Abouchami, W., Galer, S. J. G., de Baar, H. J. W., Alderkamp, A. C., Middag, R., Laan, P., Andreae, M. O. (2011). Modulation of the Southern Ocean cadmium isotope signature by ocean circulation and primary productivity. *Earth and Planetary Science Letters*, *305*(1-2), 83–91. https://doi.org/10.1016/j.epsl.2011.02.044

Abouchami, W., Galer, S. J. G., de Baar, H. J. W., Middag, R., Vance, D., Zhao, Y., Andreae, M. O. (2014). Biogeochemical cycling of cadmium isotopes in the Southern Ocean along the Zero Meridian. *Geochimica et Cosmochimica Acta*, *127*, 348–367. https://doi.org/10.1016/j.gca.2013.10.022

Abouchami, W., Galer, S. J. G., Horner, T. J., Rehkämper, M., Wombacher, F., Xue, Z., Holdship, P. F. (2012). A Common Reference Material for Cadmium Isotope Studies - NIST SRM 3108. *Geostandards and Geoanalytical Research*, *37*(1), 5–17. https://doi.org/10.1111/j.1751-908x.2012.00175.x

Adriano, D. C., & Myilibrary. (2001). *Trace elements in terrestrial environments : biogeochemistry, bioavailability, and risks of metals*. New York: Springer.

Alejandro, D., & Paloma Raquel Aragon. (2012). *Trace elements : environmental sources, geochemistry and human health*. New York: Nova Publishers, Cop.

Appel, C., Ma, L. Q., Dean Rhue, R., & Kennelley, E. (2003). Point of zero charge determination in soils and minerals via traditional methods and detection of electroacoustic mobility. *Geoderma*, *113*(1-2), 77–93. https://doi.org/10.1016/s0016-7061(02)00316-6

Arora, A. K. (2018). Metal/Mixed Metal Oxides and Their Applications as Sensors: A

Review. *Asian Journal of Research in Chemistry*, *11*(2), 497. https://doi.org/10.5958/0974-4150.2018.00089.5

Aroua, M. K., Leong, S. P. P., Teo, L. Y., Yin, C. Y., & Daud, W. M. A. W. (2008). Real-time determination of kinetics of adsorption of lead(II) onto palm shell-based activated carbon using ion selective electrode. *Bioresource Technology*, *99*(13), 5786–5792. https://doi.org/10.1016/j.biortech.2007.10.010

Asuquo, E., Martin, A., Nzerem, P., Siperstein, F., & Fan, X. (2017). Adsorption of Cd(II) and Pb(II) ions from aqueous solutions using mesoporous activated carbon adsorbent: Equilibrium, kinetics and characterisation studies. *Journal of Environmental Chemical Engineering*, *5*(1), 679–698. https://doi.org/10.1016/j.jece.2016.12.043

Baskaran, M. (2011). *Handbook of environmental isotope geochemistry*. Heidelberg Germany ; New York: Springer.

Bazarkina, E. F., Pokrovski, G. S., Zotov, A. V., & Hazemann, J.-L. (2010). Structure and stability of cadmium chloride complexes in hydrothermal fluids. *Chemical Geology*, *276*(1-2), 1–17. https://doi.org/10.1016/j.chemgeo.2010.03.006

Benjamin, M. M., & Leckie, J. O. (1981). Multiple-site adsorption of Cd, Cu, Zn, and Pb on amorphous iron oxyhydroxide. *Journal of Colloid and Interface Science*, *79*(1), 209–221. https://doi.org/10.1016/0021-9797(81)90063-1

Bhongale, S. R., Ingawale, H. R., Shinde, T. J., & Vasambekar, P. N. (2018). Effect of Nd 3+ substitution on structural and magnetic properties of Mg–Cd ferrites synthesized by microwave sintering technique. *Journal of Rare Earths*, *36*(4), 390–397. https://doi.org/10.1016/j.jre.2017.11.003

Bowles, J. F. W. (2021). *Encyclopedia of Geology (Second Edition)* (Vol. 1).

Bryan, A. L., Dong, S., Wilkes, E. B., & Wasylenki, L. E. (2015). Zinc isotope fractionation during adsorption onto Mn oxyhydroxide at low and high ionic strength.

Geochimica et Cosmochimica Acta, *157*, 182–197. https://doi.org/10.1016/j.gca.2015.01.026

Bürger, R., Concha, F., & Tiller, F. M. (2000). Applications of the phenomenological theory to several published experimental cases of sedimentation processes. *Chemical Engineering Journal*, *80*(1-3), 105–117. https://doi.org/10.1016/s1383-5866(00)00090-3

Cao, J., Xue, H., & Sigg, L. (2006). Effects of pH and Ca competition on complexation of cadmium by fulvic acids and by natural organic ligands from a river and a lake. *Aquatic Geochemistry*, *12*(4), 375–387. https://doi.org/10.1007/s10498-006-9004-6

Cappuyns, V., & Swennen, R. (2008). "Acid extractable" metal concentrations in solid matrices: A comparison and evaluation of operationally defined extraction procedures and leaching tests. *Talanta*, *75*(5), 1338–1347. https://doi.org/10.1016/j.talanta.2008.01.047

Chen, Y., Peng, L., Zeng, Q., Yang, Y., Lei, M., Song, H., Gu, J. (2014). Removal of trace Cd(II) from water with the manganese oxides/ACF composite electrode. *Clean Technologies and Environmental Policy*, *17*(1), 49–57. https://doi.org/10.1007/s10098-014-0756-1

Chen, Z., Zhang, J., Fu, J., Wang, M., Wang, X., Han, R., & Xu, Q. (2014). Adsorption of methylene blue onto poly(cyclotriphosphazene-co-4,4′-sulfonyldiphenol) nanotubes: Kinetics, isotherm and thermodynamics analysis. *Journal of Hazardous Materials*, *273*, 263–271. https://doi.org/10.1016/j.jhazmat.2014.03.053

Chisholm-Brause, C. J., O'Day, P. A., Brown, G. E., & Parks, G. A. (1990). Evidence for multinuclear metal-ion complexes at solid/water interfaces from X-ray absorption spectroscopy. *Nature*, *348*(6301), 528–531. https://doi.org/10.1038/348528a0

Chrastný, V., Čadková, E., Vaněk, A., Teper, L., Cabala, J., & Komárek, M. (2015). Cadmium isotope fractionation within the soil profile complicates source identification in relation to Pb–Zn mining and smelting processes. *Chemical Geology*, *405*, 1–9. https://doi.org/10.1016/j.chemgeo.2015.04.002

Chuanwei, Z., Hanjie, W., Yuxu, Z., Yizhang, L., & Rongfei, W. (2015). Isotopic Geochemistry of Cadmium: A Review. *Acta Geologica Sinica - English Edition*, *89*(6), 2048–2057. https://doi.org/10.1111/1755-6724.12616

Conrad, C. F., Fugate, D., Daus, J., Chisholm-Brause, C. J., & Kuehl, S. A. (2007). Assessment of the historical trace metal contamination of sediments in the Elizabeth River, Virginia. *Marine Pollution Bulletin*, *54*(4), 385–395. https://doi.org/10.1016/j.marpolbul.2006.11.005

Cornell, R. M., & Udo Schwertmann. (2003). *The iron oxides : structure, properties, reactions, occurrences and uses*. Weinheim: Wiley-Vch.

Cullen, J. T., Lane, T. W., Morel, F. M. M., & Sherrell, R. M. (1999). Modulation of cadmium uptake in phytoplankton by seawater CO2 concentration. *Nature*, *402*(6758), 165–167. https://doi.org/10.1038/46007

Cullen, jay T., & Maldonado, M. T. (2013). Biogeochemistry of Cadmium and Its Release to the Environment. *Metal Ions in Life Science*, *11*, 31–62. https://doi.org/10.1007/978-94-007-5179-8_2

Dawadi, S., Gupta, A., Khatri, M., Budhathoki, B., Lamichhane, G., & Parajuli, N. (2020). Manganese dioxide nanoparticles: synthesis, application and challenges. *Bulletin of Materials Science*, *43*(1). https://doi.org/10.1007/s12034-020-02247-8

De Miguel, E., Mingot, J., Chacón, E., & Charlesworth, S. (2012). The relationship between soil geochemistry and the bioaccessibility of trace elements in playground soil. *Environmental Geochemistry and Health*, *34*(6), 677–687. https://doi.org/10.1007/s10653-012-9486-7

Della Puppa, L., Komárek, M., Bordas, F., Bollinger, J.-C., & Joussein, E. (2013). Adsorption of copper, cadmium, lead and zinc onto a synthetic manganese oxide. *Journal of Colloid and Interface Science*, *399*, 99–106. https://doi.org/10.1016/j.jcis.2013.02.029

Deng, Y., Huang, S., Dong, C., Meng, Z., & Wang, X. (2020). Competitive adsorption behaviour and mechanisms of cadmium, nickel and ammonium from aqueous solution by fresh and ageing rice straw biochars. *Bioresource Technology*, *303*, 122853. https://doi.org/10.1016/j.biortech.2020.122853

Deveci, H., & Kar, Y. (2013). Adsorption of hexavalent chromium from aqueous solutions by bio-chars obtained during biomass pyrolysis. *Journal of Industrial and Engineering Chemistry*, *19*(1), 190–196. https://doi.org/10.1016/j.jiec.2012.08.001

Douven, S., Paez, C. A., & Gommes, C. J. (2015). The range of validity of sorption kinetic models. *Journal of Colloid and Interface Science*, *448*, 437–450. https://doi.org/10.1016/j.jcis.2015.02.053

Durante-Yánez, E. V., Martínez-Macea, M. A., Enamorado-Montes, G., Combatt Caballero, E., & Marrugo-Negrete, J. (2022). Phytoremediation of Soils Contaminated with Heavy Metals from Gold Mining Activities Using Clidemia sericea D. Don. *Plants*, *11*(5), 597. https://doi.org/10.3390/plants11050597

Dziubanek, G., Piekut, A., Rusin, M., Baranowska, R., & Hajok, I. (2015). Contamination of food crops grown on soils with elevated heavy metals content. *Ecotoxicology and Environmental Safety*, *118*, 183–189. https://doi.org/10.1016/j.ecoenv.2015.04.032

Ekman, R., Jerzy Silberring, Westman-Brinkmalm, A., & Agnieszka Kraj. (2008). *Mass Spectrometry Instrumentation, Interpretation, and Applications*. Hoboken, Nj, Usa John Wiley & Sons, Inc.

El-Khaiary, M. I., & Malash, G. F. (2011). Common data analysis errors in batch adsorption studies. *Hydrometallurgy*, *105*(3-4), 314–320. https://doi.org/10.1016/j.hydromet.2010.11.005

Engelhard, M. H., Droubay, T. C., & Du, Y. (2017). *X-Ray photoelectron Spectroscopy Applications*. Retrieved from https://doi.org/10.1016/B978-0-12-409547-2.12102-X

Ettler, V., Knytl, V., Komárek, M., Puppa, L. D., Bordas, F., Mihaljevič, M., Šebek, O. (2014). Stability of a novel synthetic amorphous manganese oxide in contrasting soils. *Geoderma*, *214-215*, 2–9. https://doi.org/10.1016/j.geoderma.2013.10.011

Farmer, A. (1997). *Managing environmental pollution*. London: Routledge, Cop.

Feng, X., Wang, Q., Sun, Y., Zhang, S., & Wang, F. (2022). Microplastics change soil properties, heavy metal availability and bacterial community in a Pb-Zn-contaminated soil. *Journal of Hazardous Materials*, *424*, 127364. https://doi.org/10.1016/j.jhazmat.2021.127364

Fernandes, M. M., & Baeyens, B. (2019). Cation exchange and surface complexation of lead on montmorillonite and illite including competitive adsorption effects. *Applied Geochemistry*, *100*, 190–202. https://doi.org/10.1016/j.apgeochem.2018.11.005

Feska, S., Muslim, & Haeruddin. (2021). A enrichment factor for cadmium and lead in sediment of Gembong estuary, Bekasi, Indonesia. *International Journal of Engineering Science Technologies*, *5*(2), 38–44. https://doi.org/10.29121/ijoest.v5.i2.2021.157

Foo, K. Y., & Hameed, B. H. (2009). A short review of activated carbon assisted electrosorption process: An overview, current stage and future prospects. *Journal of Hazardous Materials*, *170*(2-3), 552–559. https://doi.org/10.1016/j.jhazmat.2009.05.057

Fulda, B., Voegelin, A., & Kretzschmar, R. (2013). Redox-Controlled Changes in

Cadmium Solubility and Solid-Phase Speciation in a Paddy Soil As Affected by Reducible Sulfate and Copper. *Environmental Science & Technology*, *47*(22), 12775–12783. https://doi.org/10.1021/es401997d

Gallego, S. M., Pena, L. B., Barcia, R. A., Azpilicueta, C. E., Iannone, M. F., Rosales, E. P., Benavides, M. P. (2012). Unravelling cadmium toxicity and tolerance in plants: Insight into regulatory mechanisms. *Environmental and Experimental Botany*, *83*, 33–46. https://doi.org/10.1016/j.envexpbot.2012.04.006

Garcia Gonzalez, M. N., Quiroga-Flores, R., & Börjesson, P. (2022). Life cycle assessment of a nanomaterial-based adsorbent developed on lab scale for cadmium removal: Comparison of the impacts of production, use and recycling. *Cleaner Environmental Systems*, *4*, 100071. https://doi.org/10.1016/j.cesys.2022.100071

Garrison Sposito. (2008). *The chemistry of soils*. New York, Ny: Oxford University Press.

Gauri Misra. (2019). *Data processing handbook for complex biological data sources*. London, United Kingdom: Academic Press.

Gräfe, M., Singh, B., & Balasubramanian, M. (2007). Surface speciation of Cd(II) and Pb(II) on kaolinite by XAFS spectroscopy. *Journal of Colloid and Interface Science*, *315*(1), 21–32. https://doi.org/10.1016/j.jcis.2007.05.022

Gramlich, A., Tandy, S., Gauggel, C., López, M., Perla, D., Gonzalez, V., & Schulin, R. (2018). Soil cadmium uptake by cocoa in Honduras. *Science of the Total Environment*, *612*, 370–378. https://doi.org/10.1016/j.scitotenv.2017.08.145

Guérin, T., Oustrière, N., Bulteel, D., Betrancourt, D., Ghinet, A., Malladi, S., Waterlot, C. (2022). Removal of heavy metals from contaminated water using industrial wastes containing calcium and magnesium. *Journal of Cleaner Production*, *337*, 130472. https://doi.org/10.1016/j.jclepro.2022.130472

Günay, A., Arslankaya, E., & Tosun, İ. (2007). Lead removal from aqueous solution by

natural and pretreated clinoptilolite: Adsorption equilibrium and kinetics. *Journal of Hazardous Materials*, *146*(1-2), 362–371. https://doi.org/10.1016/j.jhazmat.2006.12.034

Guo, H., & Barnard, A. S. (2013). Naturally occurring iron oxide nanoparticles: morphology, surface chemistry and environmental stability. *J. Mater. Chem. A*, *1*(1), 27–42. https://doi.org/10.1039/c2ta00523a

Hamid, Y., Tang, L., Hussain, B., Usman, M., Liu, L., Cao, X., Yang, X. (2020). Cadmium mobility in three contaminated soils amended with different additives as evaluated by dynamic flow-through experiments. *Chemosphere*, *261*, 127763. https://doi.org/10.1016/j.chemosphere.2020.127763

Hao, Y.-M., Man, C., & Hu, Z.-B. (2010). Effective removal of Cu (II) ions from aqueous solution by amino-functionalized magnetic nanoparticles. *Journal of Hazardous Materials*, *184*(1-3), 392–399. https://doi.org/10.1016/j.jhazmat.2010.08.048

Hayes, K. F., Roe, A. L., Brown, G. E., Hodgson, K. O., Leckie, J. O., & Parks, G. A. (1987). In Situ X-ray Absorption Study of Surface Complexes: Selenium Oxyanions on α-FeOOH. *Science*, *238*(4828), 783–786. https://doi.org/10.1126/science.238.4828.783

Ho, Y.-S. (2006). Second-order kinetic model for the sorption of cadmium onto tree fern: A comparison of linear and non-linear methods. *Water Research*, *40*(1), 119–125. https://doi.org/10.1016/j.watres.2005.10.040

Hoefs, J., & Springerlink (Online Service. (2015). *Stable Isotope Geochemistry*. Cham: Springer International Publishing.

Holbrook, R. D., Galyean, A. A., Gorham, J. M., Herzing, A., & Pettibone, J. (2015). Overview of Nanomaterial Characterization and Metrology. *In Frontiers of Nanoscience Elsevier*, *8*, 47–87.

Holden, N. E., Coplen, T. B., Böhlke, J. K., Tarbox, L. V., Benefield, J., Laeter, J. R. de,

Yoneda, S. (2018). IUPAC Periodic Table of the Elements and Isotopes (IPTEI) for the Education Community (IUPAC Technical Report). *Pure and Applied Chemistry*, *90*(12), 1833–2092. https://doi.org/10.1515/pac-2015-0703

Houben, D., Evrard, L., & Sonnet, P. (2013). Mobility, bioavailability and pH-dependent leaching of cadmium, zinc and lead in a contaminated soil amended with biochar. *Chemosphere*, *92*(11), 1450–1457. https://doi.org/10.1016/j.chemosphere.2013.03.055

Hua, M., Zhang, S., Pan, B., Zhang, W., Lv, L., & Zhang, Q. (2012). Heavy metal removal from water/wastewater by nanosized metal oxides: A review. *Journal of Hazardous Materials*, *211-212*, 317–331. https://doi.org/10.1016/j.jhazmat.2011.10.016

Imseng, M., Wiggenhauser, M., Keller, A., Müller, M., Rehkämper, M., Murphy, K., Bigalke, M. (2018). Towards an understanding of the Cd isotope fractionation during transfer from the soil to the cereal grain. *Environmental Pollution*, *244*, 834–844. https://doi.org/10.1016/j.envpol.2018.09.149

Isaure, M.-P., Huguet, S., Meyer, C.-L., Castillo-Michel, H., Testemale, D., Vantelon, D., Sarret, G. (2015). Evidence of various mechanisms of Cd sequestration in the hyperaccumulator Arabidopsis halleri, the non-accumulator Arabidopsis lyrata, and their progenies by combined synchrotron-based techniques. *Journal of Experimental Botany*, *66*(11), 3201–3214. https://doi.org/10.1093/jxb/erv131

Jefferson, T. (2022, March 29). It's Elemental - The Element Cadmium. Retrieved March 28, 2022, from education.jlab.org website: https://education.jlab.org/itselemental/iso048.html

Jiraungkoorskul, K., Arphorn, S., Tipayamongholgul, M., & Siriwong, W. (2016). Cadmium Contamination in Farmland Soil and Water Near Zinc Mining Site. *Kesmas: National Public Health Journal*, *10*(3), 99.

https://doi.org/10.21109/kesmas.v10i3.945

Johnston, R. L. (2012). Metal nanoparticles and nano alloys. *In Frontiers of Nano Science*, *3*, 1–42. Retrieved from Elsevier.

Jossens, L., Prausnitz, J. M., Fritz, W., Schlünder, E. U., & Myers, A. L. (1978). Thermodynamics of multi-solute adsorption from dilute aqueous solutions. *Chemical Engineering Science*, *33*(8), 1097–1106. https://doi.org/10.1016/0009-2509(78)85015-5

Juillot, F., Maréchal, C., Ponthieu, M., Cacaly, S., Morin, G., Benedetti, M., Guyot, F. (2008). Zn isotopic fractionation caused by sorption on goethite and 2-Lines ferrihydrite. *Geochimica et Cosmochimica Acta*, *72*(19), 4886–4900. https://doi.org/10.1016/j.gca.2008.07.007

Karlsson, T., Persson, P., & Skyllberg, U. (2005). Extended X-ray Absorption Fine Structure Spectroscopy Evidence for the Complexation of Cadmium by Reduced Sulfur Groups in Natural Organic Matter. *Environmental Science & Technology*, *39*(9), 3048–3055. https://doi.org/10.1021/es048585a

Khalid, S., Shahid, M., Niazi, N. K., Murtaza, B., Bibi, I., & Dumat, C. (2017). A comparison of technologies for remediation of heavy metal contaminated soils. *Journal of Geochemical Exploration*, *182*, 247–268. https://doi.org/10.1016/j.gexplo.2016.11.021

Kinuthia, G. K., Ngure, V., Beti, D., Lugalia, R., Wangila, A., & Kamau, L. (2020). Levels of heavy metals in wastewater and soil samples from open drainage channels in Nairobi, Kenya: community health implication. *Scientific Reports*, *10*(1), 8434. https://doi.org/10.1038/s41598-020-65359-5

Kirkland, K. (2007). *Particles and the universe*. New York Ny: Facts On File, Inc.

Komárek, M., Antelo, J., Králová, M., Veselská, V., Číhalová, S., Chrastný, V., Koretsky, C. M. (2018). Revisiting models of Cd, Cu, Pb and Zn adsorption onto Fe(III)

oxides. *Chemical Geology*, *493*, 189–198. https://doi.org/10.1016/j.chemgeo.2018.05.036

Komárek, M., Ettler, V., Száková, J., Šebek, O., & Tlustoš, P. (2009). Bioavailability of Lead and Cadmium in Soils Artificially Contaminated with Smelter Fly Ash. *Bulletin of Environmental Contamination and Toxicology*, *83*(2), 286–290. https://doi.org/10.1007/s00128-009-9742-4

Komárek, M., Koretsky, C. M., Stephen, K. J., Alessi, D. S., & Chrastný, V. (2015). Competitive Adsorption of Cd(II), Cr(VI), and Pb(II) onto Nanomaghemite: A Spectroscopic and Modeling Approach. *Environmental Science & Technology*, *49*(21), 12851–12859. https://doi.org/10.1021/acs.est.5b03063

Komárek, M., Ratié, G., Vaňková, Z., Šípková, A., & Chrastný, V. (2021). Metal isotope complexation with environmentally relevant surfaces: Opening the isotope fractionation black box. *Critical Reviews in Environmental Science and Technology*, 1–31. https://doi.org/10.1080/10643389.2021.1955601

Koretsky, C. (2000). The significance of surface complexation reactions in hydrologic systems: a geochemist's perspective. *Journal of Hydrology*, *230*(3-4), 127–171. https://doi.org/10.1016/s0022-1694(00)00215-8

Kumar, A., Subrahmanyam, G., Mondal, R., Cabral-Pinto, M. M. S., Shabnam, A. A., Jigyasu, D. K., Yu, Z.-G. (2021). Bio-remediation approaches for alleviation of cadmium contamination in natural resources. *Chemosphere*, *268*, 128855. https://doi.org/10.1016/j.chemosphere.2020.128855

Kumar, S., J. Shinde, T., & N. Vasambekar, P. (2013). Microwave Synthesis And Characterization Of Nanocrystalline Mn-Zn Ferrites. *Advanced Materials Letters*, *4*(5), 373–377. https://doi.org/10.5185/amlett.2012.10429

Kyzas, G. Z., Siafaka, P. I., Pavlidou, E. G., Chrissafis, K. J., & Bikiaris, D. N. (2015). Synthesis and adsorption application of succinyl-grafted chitosan for the

simultaneous removal of zinc and cationic dye from binary hazardous mixtures. *Chemical Engineering Journal*, *259*, 438–448. https://doi.org/10.1016/j.cej.2014.08.019

Largitte, L., & Pasquier, R. (2016). A review of the kinetics adsorption models and their application to the adsorption of lead by an activated carbon. *Chemical Engineering Research and Design*, *109*, 495–504. https://doi.org/10.1016/j.cherd.2016.02.006

Lashen, Z. M., Shams, M. S., El-Sheshtawy, H. S., Slaný, M., Antoniadis, V., Yang, X., Elmahdy, S. M. (2022). Remediation of Cd and Cu contaminated water and soil using novel nanomaterials derived from sugar beet processing- and clay brick factory-solid wastes. *Journal of Hazardous Materials*, *428*, 128205. https://doi.org/10.1016/j.jhazmat.2021.128205

Leiva, C. A., Gálvez, M. E., Fuentes, G. E., Acuña, C. A., & Alcota, J. A. (2022). Effects of Various Precipitants on Iron Removal from a Zinc Concentrate Pressure Leaching Solution. *Minerals*, *12*(1), 84. https://doi.org/10.3390/min12010084

Li, D., & Kaplan, D. I. (2012). Sorption coefficients and molecular mechanisms of Pu, U, Np, Am and Tc to Fe (hydr)oxides: A review. *Journal of Hazardous Materials*, *243*, 1–18. https://doi.org/10.1016/j.jhazmat.2012.09.011

Li, J., Zhang, S., & Ding, X. (2022). The combined application of biochar and high phosphate fertilizer promoted the mobilization and redistribution of cadmium in rhizosphere soil. *Journal of Environmental Chemical Engineering*, *10*(3), 107482. https://doi.org/10.1016/j.jece.2022.107482

Li, X., Zheng, W., Wang, D., Yang, Q., Cao, J., Yue, X., Zeng, G. (2010). Removal of Pb (II) from aqueous solutions by adsorption onto modified areca waste: Kinetic and thermodynamic studies. *Desalination*, *258*(1-3), 148–153. https://doi.org/10.1016/j.desal.2010.03.023

Liu, C., & Huang, P. M. (2003). Kinetics of lead adsorption by iron oxides formed under the influence of citrate. *Geochimica et Cosmochimica Acta*, *67*(5), 1045–1054. https://doi.org/10.1016/s0016-7037(02)01036-0

Loganathan P., Vigneswaran, S., Kandasamy, J., & Naidu R. (2012). Cadmium Sorption and Desorption in Soils: A Review. *Critical Reviews in Environmental Science and Technology*, *42*(5), 489–533. https://doi.org/10.1080/10643389.2010.520234

Macfarlane, A. L., Prestidge, R., Farid, M. M., & Chen, J. J. J. (2009). Dissolved air flotation: A novel approach to recovery of organosolv lignin. *Chemical Engineering Journal*, *148*(1), 15–19. https://doi.org/10.1016/j.cej.2008.07.036

Mather R.R. (2009). *Surface modification of textiles by plasma treatments*. Elsevier Inc.

Michálková, Z., Komárek, M., Vítková, M., Řečínská, M., & Ettler, V. (2016). Stability, transformations and stabilizing potential of an amorphous manganese oxide and its surface-modified form in contaminated soils. *Applied Geochemistry*, *75*, 125–136. https://doi.org/10.1016/j.apgeochem.2016.10.020

Michener, R. H., & Lajtha, K. (2007). *Stable isotopes in ecology and environmental science*. Malden, Mass.: Blackwell Pub.

Miller, M. A., Petrasch, J., Randhir, K., Rahmatian, N., & Klausner, J. (2021). Chemical Energy Storage In Thermal, Mechanical, and Hybrid Chemical Energy Storage Systems. *Academic Press*, 249–292.

Mo, X., Siebecker, M. G., Gou, W., Li, L., & Li, W. (2021). A review of cadmium sorption mechanisms on soil mineral surfaces revealed from synchrotron-based X-ray absorption fine structure spectroscopy: Implications for soil remediation. *Pedosphere*, *31*(1), 11–27. https://doi.org/10.1016/s1002-0160(20)60017-0

Moiseenko, T. I., & Gashkina, N. A. (2018). Biogeochemistry of Cadmium: Anthropogenic Dispersion, Bioaccumulation, and Ecotoxicity. *Geochemistry International*, *56*(8), 798–811. https://doi.org/10.1134/s0016702918080062

Morais da Silva, P. M., Camparotto, N. G., Grego Lira, K. T., Franco Picone, C. S., & Prediger, P. (2020). Adsorptive removal of basic dye onto sustainable chitosan beads: Equilibrium, kinetics, stability, continuous-mode adsorption and mechanism. *Sustainable Chemistry and Pharmacy*, *18*, 100318. https://doi.org/10.1016/j.scp.2020.100318

Navarro-León, E., Oviedo-Silva, J., Ruiz, J. M., & Blasco, B. (2019). Possible role of HMA4a TILLING mutants of Brassica rapa in cadmium phytoremediation programs. *Ecotoxicology and Environmental Safety*, *180*, 88–94. https://doi.org/10.1016/j.ecoenv.2019.04.081

Nazari, M., & Halladj, R. (2014). Adsorptive removal of fluoride ions from aqueous solution by using sonochemically synthesized nanomagnesia/alumina adsorbents: An experimental and modeling study. *Journal of the Taiwan Institute of Chemical Engineers*, *45*(5), 2518–2525. https://doi.org/10.1016/j.jtice.2014.05.020

Neville, A,, Mather R.R, & J.I.B, W. (2007). *Characterisation of plasma-treated textiles*. Elsevier Ltd.

Ogata, F., Nagahashi, E., Miki, H., Saenjum, C., Nakamura, T., & Kawasaki, N. (2020). Assessment of Cd(II) adsorption capability and mechanism from aqueous phase using virgin and calcined lignin. *Heliyon*, *6*(6), e04298. https://doi.org/10.1016/j.heliyon.2020.e04298

Omar, S., Muhamad, M. S., Te Chuan, L., Hadibarata, T., & Teh, Z. C. (2019). A Review on Lead Sources, Occurrences, Health Effects, and Treatment Using Hydroxyapatite (HAp) Adsorbent Made from Fish Waste. *Water, Air, & Soil Pollution*, *230*(12). https://doi.org/10.1007/s11270-019-4312-9

Ouředníček, P., Hudcová, B., Trakal, L., Pohořelý, M., & Komárek, M. (2019). Synthesis of modified amorphous manganese oxide using low-cost sugars and biochars:

Material characterization and metal(loid) sorption properties. *Science of the Total Environment*, *670*, 1159–1169. https://doi.org/10.1016/j.scitotenv.2019.03.300

Page, A. L., & Bingham, F. T. (1973). Cadmium residues in the environment. *Residue Reviews*, *48(0)*, 1–44. https://doi.org/10.1007/978-1-4615-8498-8_1

Paterson, E. (2000). U. Schwertmann & R.M. Cornell. Iron Oxides in the Laboratory. Preparation and Characterization. VCH, Weinheim, 1991. xiv + 137 pp. Price £45 ISBN: 3.527.26991.6. *Clay Minerals*, *27*(3), 393–393. https://doi.org/10.1180/claymin.1992.027.3.14

Peacock, C. L., & Sherman, D. M. (2004). Copper(II) sorption onto goethite, hematite and lepidocrocite: a surface complexation model based on ab initio molecular geometries and EXAFS spectroscopy. *Geochimica et Cosmochimica Acta*, *68*(12), 2623–2637. https://doi.org/10.1016/j.gca.2003.11.030

Perez-Chaca, M., V., Rodriguez-Serrano, M., Molina, A. S., Pedranzani, H. E., Zirulnik, F., Sandalio, L. M., & Rpmero-Puertas, M. C. (2014). Cadmium induces two waves of reactive oxygen species inGlycine max(L.) roots. *Plant, Cell & Environment*, *37*(7), 1672–1687. https://doi.org/10.1111/pce.12280

Phillips, D. J. H. (1995). The chemistries and environmental fates of trace metals and organochlorines in aquatic ecosystems. *Marine Pollution Bulletin*, *31*(4-12), 193–200. https://doi.org/10.1016/0025-326x(95)00194-r

PicóY. (2015). *Advanced mass spectrometry for food safety and quality*. Amsterdam, Netherlands: Elsevier.

Plazinski, W., Rudzinski, W., & Plazinska, A. (2009). Theoretical models of sorption kinetics including a surface reaction mechanism: A review. *Advances in Colloid and Interface Science*, *152*(1-2), 2–13. https://doi.org/10.1016/j.cis.2009.07.009

Post, J. E. (1999). Manganese oxide minerals: Crystal structures and economic and environmental significance. *Proceedings of the National Academy of Sciences*,

96(7), 3447–3454. https://doi.org/10.1073/pnas.96.7.3447

Prohaska, T., & Al, E. (2015). *Sector field mass spectrometry for elemental and isotopic analysis*. Cambridge: The Royal Society Of Chemistry, Cop.

Ratié, G., Chrastný, V., Guinoiseau, D., Marsac, R., Vaňková, Z., & Komárek, M. (2021). Cadmium Isotope Fractionation during Complexation with Humic Acid. *Environmental Science & Technology*, *55*(11), 7430–7444. https://doi.org/10.1021/acs.est.1c00646

Rizwan, M., Ali, S., Zia ur Rehman, M., Rinklebe, J., Tsang, D. C. W., Bashir, A., Ok, Y. S. (2018). Cadmium phytoremediation potential of Brassica crop species: A review. *Science of the Total Environment*, *631-632*, 1175–1191. https://doi.org/10.1016/j.scitotenv.2018.03.104

Robert Peter Mason, & Wiley, J. (2013). *Trace metals in aquatic systems*. Chichester: Wiley-Blackwell/John Wiley & Sons, Cop.

Robson, T. C., Braungardt, C. B., Rieuwerts, J., & Worsfold, P. (2014). Cadmium contamination of agricultural soils and crops resulting from sphalerite weathering. *Environmental Pollution*, *184*, 283–289. https://doi.org/10.1016/j.envpol.2013.09.001

Rudzinski, W., & Plazinski, W. (2007). Studies of the Kinetics of Solute Adsorption at Solid/Solution Interfaces: On the Possibility of Distinguishing between the Diffusional and the Surface Reaction Kinetic Models by Studying the Pseudo-First-order Kinetics. *The Journal of Physical Chemistry C*, *111*(41), 15100–15110. https://doi.org/10.1021/jp073249c

Satarug, S., Baker, J. R., Urbenjapol, S., Haswell-Elkins, M., Reilly, P. E. B., Williams, D. J., & Moore, M. R. (2003). A global perspective on cadmium pollution and toxicity in non-occupationally exposed population. *Toxicology Letters*, *137*(1-2), 65–83. https://doi.org/10.1016/s0378-4274(02)00381-8

Scheidegger, A. M., Lamble, G. M., & Sparks, D. L. (1996). Investigation of Ni Sorption on Pyrophyllite: An XAFS Study. *Environmental Science & Technology*, *30*(2), 548–554. https://doi.org/10.1021/es950293+

Schmitt, A.-D. (2009). High-precision cadmium stable isotope measurements by double spike thermal ionisation mass spectrometry. *Journal of Analytical Atomic Spectrometry*, *24*(8), 1079. https://doi.org/10.1039/b821576f

Schmitt, A.-D., Galer, S. J. G., & Abouchami, W. (2009). High-precision cadmium stable isotope measurements by double spike thermal ionisation mass spectrometry. *Journal of Analytical Atomic Spectrometry*, *24*(8), 1079. https://doi.org/10.1039/b821576f

Schwertmann, U., & Fechter, H. (1982). The point of zero charge of natural and synthetic ferrihydrites and its relation to adsorbed silicate. *Clay Minerals*, *17*(4), 471–476. https://doi.org/10.1180/claymin.1982.017.4.10

Shahid, M., Dumat, C., Khalid, S., Schreck, E., Xiong, T., & Niazi, N. K. (2017). Foliar heavy metal uptake, toxicity and detoxification in plants: A comparison of foliar and root metal uptake. *Journal of Hazardous Materials*, *325*, 36–58. https://doi.org/10.1016/j.jhazmat.2016.11.063

Sharma, G., Kumar, A., Ghfar, A. A., García-Peñas, A., Naushad, Mu., & Stadler, F. J. (2021). Fabrication and Characterization of Xanthan Gum-cl-poly(acrylamide-co-alginic acid) Hydrogel for Adsorption of Cadmium Ions from Aqueous Medium. *Gels*, *8*(1), 23. https://doi.org/10.3390/gels8010023

Shi, M., Min, X., Ke, Y., Lin, Z., Yang, Z., Wang, S., Wei, Y. (2021). Recent progress in understanding the mechanism of heavy metals retention by iron (oxyhydr)oxides. *Science of the Total Environment*, *752*, 141930. https://doi.org/10.1016/j.scitotenv.2020.141930

Spurgeon, S. R., Du, Y., & Chambers, S. A. (2017). Measurement Error in Atomic-Scale

Scanning Transmission Electron Microscopy—Energy-Dispersive X-Ray Spectroscopy (STEM-EDS) Mapping of a Model Oxide Interface. *Microscopy and Microanalysis*, *23*(3), 513–517. https://doi.org/10.1017/s1431927617000368

Stigliani, W. M., Doelman, P., Salomons, W., Schulin, R., Smidt, G. R. B., & Van der Zee, S. E. A. T. M. (1991). Chemical Time Bombs: Predicting the Unpredictable. *Environment: Science and Policy for Sustainable Development*, *33*(4), 4–30. https://doi.org/10.1080/00139157.1991.9931383

Strawn. (2015). *Soil Chemistry 5Th Edition.*

Strawn, D. G., Bohn, H. L., & O'Connor, G. A. (2020). *Soil Chemistry 5Th Edition.* (5th ed.). Wiley-Blackwell.

Tchobanoglous, G., & Eddy, M. (2003). *Wastewater engineering : treatment and resource recovery. Volume 1.* Boston: Mcgraw-Hill.

Teng, F.-Z., Dauphas, N., & Watkins, J. M. (2017). Non-Traditional Stable Isotopes: Retrospective and Prospective. *Reviews in Mineralogy and Geochemistry*, *82*(1), 1–26. https://doi.org/10.2138/rmg.2017.82.1

Trakal, L., Michálková, Z., Beesley, L., Vítková, M., Ouředníček, P., Barceló, A. P., Komárek, M. (2018). AMOchar: Amorphous manganese oxide coating of biochar improves its efficiency at removing metal(loid)s from aqueous solutions. *Science of the Total Environment*, *625*, 71–78. https://doi.org/10.1016/j.scitotenv.2017.12.267

Vaněk, A., Borůvka, L., Drábek, O., Mihaljevič, M., & Komárek, M. (2005). Mobility of lead, zinc and cadmium in alluvial soils heavily polluted by smelting industry. *Plant, Soil and Environment*, *51*(No, 7), 316–321. https://doi.org/10.17221/3592-pse

Vinh, N. D., Thao, P. T. P., & Hanh, N. T. (2019). Feasibility of goethite nanoparticles for Pb(II) and Cd(II) removal from aqueous solution. *Vietnam Journal of Chemistry*,

57(3), 281–287. https://doi.org/10.1002/vjch.201960027

Vítková, M., Puschenreiter, M., & Komárek, M. (2018). Effect of nano zero-valent iron application on As, Cd, Pb, and Zn availability in the rhizosphere of metal(loid) contaminated soils. *Chemosphere*, *200*, 217–226. https://doi.org/10.1016/j.chemosphere.2018.02.118

Vodyanitskii, Yu. N., & Shoba, S. A. (2016). Ferrihydrite in soils. *Eurasian Soil Science*, *49*(7), 796–806. https://doi.org/10.1134/s1064229316070127

Wang, F., Zhang, X., Zhang, S., Zhang, S., & Sun, Y. (2020). Interactions of microplastics and cadmium on plant growth and arbuscular mycorrhizal fungal communities in an agricultural soil. *Chemosphere*, *254*, 126791. https://doi.org/10.1016/j.chemosphere.2020.126791

Wang, M., Chen, S., Shi, H., & Liu, Y. (2022). Redox dependence of manganese controls cadmium isotope fractionation in a paddy soil-rice system under unsteady pe + pH conditions. *Science of the Total Environment*, *806*, 150675. https://doi.org/10.1016/j.scitotenv.2021.150675

Wasylenki, L. E., Swihart, J. W., & Romaniello, S. J. (2014). Cadmium isotope fractionation during adsorption to Mn oxyhydroxide at low and high ionic strength. *Geochimica et Cosmochimica Acta*, *140*, 212–226. https://doi.org/10.1016/j.gca.2014.05.007

Wei, S., Li, D., Huang, Z., Huang, Y., & Wang, F. (2013). High-capacity adsorption of Cr(VI) from aqueous solution using a hierarchical porous carbon obtained from pig bone. *Bioresource Technology*, *134*, 407–411. https://doi.org/10.1016/j.biortech.2013.02.040

White, W. M. (2014). *Isotope geochemistry*. Chichester: Wiley Blackwell, Cop.

White, W. M. (2017). *Encyclopedia of Geochemistry*. Cham Springer International Publishing.

Wiederhold, J. G. (2015). Metal Stable Isotope Signatures as Tracers in Environmental Geochemistry. *Environmental Science & Technology*, *49*(5), 2606–2624. https://doi.org/10.1021/es504683e

Wiggenhauser, M., Bigalke, M., Imseng, M., Keller, A., Rehkämper, M., Wilcke, W., & Frossard, E. (2018). Using isotopes to trace freshly applied cadmium through mineral phosphorus fertilization in soil-fertilizer-plant systems. *Science of the Total Environment*, *648*, 779–786. https://doi.org/10.1016/j.scitotenv.2018.08.127

Wiley, J. (2022). Electron Ionization - Mass Spectrometry - ppt download. Retrieved March 28, 2022, from slideplayer.com website: https://slideplayer.com/slide/16088473/

Wilschefski, S. C., & Baxter, M. R. (2019). Inductively Coupled Plasma Mass Spectrometry: Introduction to Analytical Aspects. *Clinical Biochemist Reviews*, *40*(3), 115–133. https://doi.org/10.33176/aacb-19-00024

Wombacher, F., Rehkämper, M., Mezger, K., & Münker, C. (2003). Stable isotope compositions of cadmium in geological materials and meteorites determined by multiple-collector ICPMS. *Geochimica et Cosmochimica Acta*, *67*(23), 4639–4654. https://doi.org/10.1016/s0016-7037(03)00389-2

Xin, X., Wei, Q., Yang, J., Yan, L., Feng, R., Chen, G., Li, H. (2012). Highly efficient removal of heavy metal ions by amine-functionalized mesoporous Fe3O4 nanoparticles. *Chemical Engineering Journal*, *184*, 132–140. https://doi.org/10.1016/j.cej.2012.01.016

Yang, J., Li, Y., Liu, S., Tian, H., Chen, C., Liu, J., & Shi, Y. (2015). Theoretical calculations of Cd isotope fractionation in hydrothermal fluids. *Chemical Geology*, *391*, 74–82. https://doi.org/10.1016/j.chemgeo.2014.10.029

Yao, S., Liu, Z., & Shi, Z. (2014). Adsorption behavior of cadmium ion onto synthetic ferrihydrite: effects of pH and natural seawater ligands. *Journal of the Iranian*

Chemical Society, *11*(6), 1545–1551. https://doi.org/10.1007/s13738-014-0425-7

Zhang, H., & Reynolds, M. (2019). Cadmium exposure in living organisms: A short review. *Science of the Total Environment*, *678*, 761–767. https://doi.org/10.1016/j.scitotenv.2019.04.395

Zhao, J., Niu, Y., Ren, B., Chen, H., Zhang, S., Jin, J., & Zhang, Y. (2018). Synthesis of Schiff base functionalized superparamagnetic Fe3O4 composites for effective removal of Pb(II) and Cd(II) from aqueous solution. *Chemical Engineering Journal*, *347*, 574–584. https://doi.org/10.1016/j.cej.2018.04.151

Zhao, Y., Li, Y., Wiggenhauser, M., Yang, J., Sarret, G., Cheng, Q. Shi, Y. (2021). Theoretical isotope fractionation of cadmium during complexation with organic ligands. *Chemical Geology*, *571*, 120178. https://doi.org/10.1016/j.chemgeo.2021.120178